similar to that for the synthesis of isostere **20**.[17] Precise stereocontrol and introduction of other functional groups at the α-position are under investigation.

Next, we investigated whether the di/tri-peptide transporter, PEPT1 recognized synthetic Phe-Gly type isosteres as substrates. PEPT1 is a membrane protein which has 12 transmembrane domains and mediates intestinal uptake of not only di-/tripeptides but also several drugs structually related to small peptides such as β-lactam antibiotics.[18] Structure−activity relationship studies of various substrates for PEPT1 have been carried out in order to apply this transporter to develop orally bio-available drugs. However precise recognition mechanisms have not been elucidated. We envisioned that alkene dipeptide isosteres would be useful tools for analysis of recognition mechanisms of PEPT1 because of their structural similarity to parent dipeptides. We also expected that the potency of dipeptide isosteres as amide bond mimetics could be evaluated by use of the PEPT1 dipeptide transport system.

The bioactivities of synthetic Phe-Gly isosteres for PEPT1 were determined by the inhibition of [^{3}H]Gly-Sar uptake in PEPT1-expressing Caco-2 cell in comparison with *trans*-amide type isosteres, **24**, **25**, and other related compounds (see the Supporting Information attached). Inhibition constants (K_i) of parent dipeptide Phe-Gly and its isosteres are shown in Table 1. *trans*-Amide equivalents **24** and **25** possessed good affinity for PEPT1 corresponding to the parent dipeptide (K_i: Phe-Gly, 0.205 mM; **24**, 0.853 mM; **25**, 1.34 mM). It is of note that affinities of the *cis*-amide equivalents **16** and **17** for PEPT1 were more than 10 times weaker than those of *trans*-isomers. These data suggest that PEPT1 predominantly recognizes *trans*-amide conformations of dipeptides. This is in good accordance with the previous report by Brandsch et al., in which PEPT1 recognized *trans*-conformation of Ala-ψ[CS−N]-Pro.[19] Conformationally flexible analogues **26** and **27** retained moderate affinity in comparison with *cis*-amide equivalents. Presumably, analogues **26** and **27** could exist as *trans*-amide-like conformers, which were favorable for the interaction with PEPT1, due to their flexibility. Contrary to our expectation, an increase of affinity by the introduction of fluoroalkene unit was not observed (**24** vs **25**). Further investigation is required for verification of the effect of fluorine as a carbonyl oxygen mimic.

Table 1. K_i Values of Phe-Gly and Various Isosteres Based on Inhibition of [^{3}H]Gly-Sar Uptake by PEPT1 in Caco-2 Cell

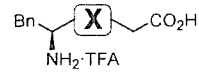

compd	X	K_i (mM)
Phe-Gly	−CO-NH−	0.205
16	−ψ[(*Z*)-CH=CH]−	>10.0
17	−ψ[(*E*)-CF=CH]−	>10.0
24	−ψ[(*E*)-CH=CH]−	0.853
25	−ψ[(*Z*)-CF=CH]−	1.34
26	−ψ[CH_2-CH_2]−	2.17
27	−ψ[CF_2-CH_2]−	1.67

In conclusion, we presented a novel unambiguous synthetic route for the syntheses of (*Z*)-alkene and (*E*)-fluoroalkene dipeptide isosteres as *cis*-amide bond mimetics via organocopper-mediated reduction of γ-acetoxy- or γ,γ-difluoro-α,β-unsaturated δ-lactams. We also carried out comparative studies of affinities for peptide transpoter PEPT1 between the *cis*-amide mimetics and the corresponding *trans*-amide isosteres, and found that peptide transporter PEPT1 predominantly recognizes *trans*-amide bond conformations in dipeptides. Synthetic studies on various α-substituted (*E*)-fluoroalkene isosteres and further structure−activity-relationship studies on dipeptide mimetics for PEPT1 are currently proceeding.

Acknowledgment. We thank Dr. Terrence R. Burke, Jr., NCI, NIH, for proofreading this manuscript. This research was supported in part by 21st Century COE Program "Knowledge Information Infrastructure for Genome Science", a Grant-in-Aid for Scientific Research from the Ministry of Education, Culture, Sports, Science and Technology, Japan, the Japan Society for the Promotion of Science (JSPS), and the Japan Health Science Foundation. A.N. is grateful for Research Fellowships from the JSPS for Young Scientists.

Supporting Information Available: Synthesis of compounds **24**−**27**. Experimental procedures and spectral data. This material is available free of charge via the Internet at http://pubs.acs.org.

OL052781K

(17) In ^{1}H NMR experiments, α-protons (position-3) of 3,6-*trans* isomers such as **18** or *trans*-**22** appeared upfield from the corresponding α-protons of 3,6-*cis* isomeres. See ref 9.

(18) (a) Våbenø, J.; Lejon, T.; Nielsen, C. U.; Steffansen, B.; Chen, W.; Ouyang, H.; Borchardt, R. T.; Luthman, K. *J. Med. Chem.* **2004**, *47*, 1060. (b) Våbenø, J.; Nielsen, C. U.; Ingebrigtsen, T.; Lejon, T.; Steffansen, B.; Luthman, K. *J. Med. Chem.* **2004**, *47*, 4755. (c) Terada, T.; Inui, K. *Curr. Drug Metab.* **2004**, *5*, 85. (d) Biegel, A.; Gebauer, S.; Hartrodt, B.; Brandsh, M.; Neubert, K.; Thondorf, I. *J. Med. Chem.* **2005**, *48*, 4410.

(19) Brandsh, M.; Thunecke, F.; Küllertz, G.; Schutkowski, M.; Fischer, G.; Neubert, K. *J. Biol. Chem.* **1998**, *273*, 3861.

Pflugers Arch - Eur J Physiol (2006) 452: 64–70
DOI 10.1007/s00424-005-0005-x

EPITHELIAL TRANSPORT

Megumi Irie · Tomohiro Terada · Masahiro Tsuda · Toshiya Katsura · Ken-ichi Inui

Prediction of glycylsarcosine transport in Caco-2 cell lines expressing PEPT1 at different levels

Received: 20 June 2005 / Accepted: 22 September 2005 / Published online: 10 November 2005

Abstract H^+-coupled peptide transporter 1 (PEPT1) and the basolateral peptide transporter mediate the absorption of small peptides and peptide-like drugs in the small intestine. Recently, we constructed a mathematical model to simulate glycylsarcosine (Gly-Sar) transport in Caco-2 cells. In this study, we attempted to adjust our model to a change in the expression level of PEPT1. To obtain cell lines expressing PEPT1 at different levels, recloning of Caco-2 cells was performed, and nine clones were isolated. Compared with parental cells, clones 1 and 9 exhibited the lowest and the highest levels of [^{14}C]Gly-Sar uptake from the apical side, respectively, whereas activities of the basolateral peptide transporter were comparable. Kinetic analysis demonstrated that the difference in the activity of PEPT1 was accounted by variations in V_{max}. Moreover, PEPT1 mRNA level was positively related to the activity of [^{14}C]Gly-Sar uptake (r=0.55). Based on these findings, the V_{max} value of PEPT1 was defined as a variable using the amount of PEPT1 mRNA as an index of the expression level. With this improved model, Gly-Sar transport in clones 1 and 9 was well-predicted, suggesting that our model can simulate Gly-Sar transport in cells expressing PEPT1 at different levels.

Keywords Peptide transporter · Small intestine · Absorption · Simulation · Expression level

Abbreviations PEPT1: H^+-coupled peptide transporter 1 · Gly-Sar: glycylsarcosine

M. Irie · T. Terada · M. Tsuda · T. Katsura · K.-i. Inui (✉)
Department of Pharmacy,
Kyoto University Hospital,
Faculty of Medicine,
Kyoto University,
Sakyo-ku,
606-8507 Kyoto, Japan
e-mail: inui@kuhp.kyoto-u.ac.jp
Tel.: +81-75-7513577
Fax: +81-75-7514207

Introduction

H^+-coupled peptide transporter 1 (PEPT1) expressed in brush-border membranes of intestinal epithelial cells transports dipeptides and tripeptides from the lumen into cells by utilizing an inward H^+ gradient and mediates the absorption of dipeptides and tripeptides [1, 6, 14, 23]. Because of its broad substrate specificity, PEPT1 can accept various peptide-like drugs, such as oral β-lactam antibiotics and the anticancer agent bestatin; therefore, PEPT1 serves as a drug transporter [7, 23, 29]. On the other hand, it has been demonstrated that another peptide transporter is expressed in the basolateral membrane [10, 12, 19, 24, 26, 27]. The basolateral peptide transporter mediates the extrusion of substrates taken up by PEPT1 into the circulation and is involved in the absorption of peptide-like drugs.

Recently, based on the influx and efflux properties of PEPT1 and the basolateral peptide transporter, we constructed a computational model of glycylsarcosine (Gly-Sar) transport in Caco-2 cells [11]. This model was composed of three compartments (i.e., the apical, cellular, and basolateral compartments) and two functional factors (PEPT1 and the basolateral peptide transporter). To reproduce the saturation of both transporters, the rate constants of Gly-Sar transport by PEPT1 and the basolateral peptide transporter were defined as variables using the respective kinetic parameters K_m and V_{max}. With this model, the time course of Gly-Sar transport at various concentrations in the absorptive direction could be predicted well, indicating that the model could be used to underlie a simulator to forecast the absorption of peptide-like drugs in the small intestine. However, the expression level of PEPT1 was presumed to be constant and was not incorporated into this model as a variable factor, although the expression level of PEPT1 differed from the segment of the intestine [17] and the intestinal PEPT1 was regulated by various factors, such as food, hormones, drugs, and diurnal rhythm [2, 23]. It is, therefore, essential to enable the model to achieve a change in the expression level of PEPT1 for the development of a simulator of drug absorption in the small intestine.

In the present study, we first performed the recloning of Caco-2 cells for two purposes: (1) to isolate clones appropriate for assessment of the improved model, and (2) to investigate the relation between transport activity and the expression level of PEPT1. Based on the findings of uptake studies and the quantification of PEPT1 mRNA, we defined the amount of PEPT1 mRNA as an index for the expression level of PEPT1, and we described mathematically the maximal velocity (V_{max}) of PEPT1. Furthermore, using two clones differing in the expression level of PEPT1, validation of the improved model of Gly-Sar transport was performed.

Materials and methods

Materials

[^{14}C]Gly-Sar (4.07 GBq/mmol) was obtained from Moravek Biochemicals, Inc. (Brea, CA, USA) and D-[1-^{3}H(N)] mannitol (629 GBq/mmol) was from NEN Life Science Products, Inc. (Boston, MA, USA). Gly-Sar was purchased from Sigma Chemical Co. (St. Louis, MO, USA). All other chemicals used were of the highest purity available.

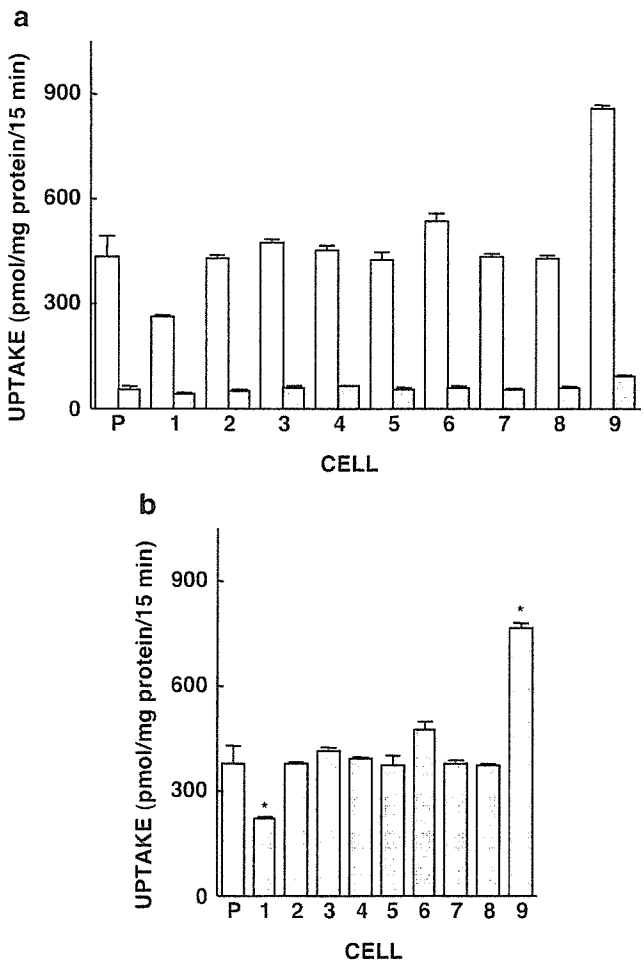

Fig. 1 [^{14}C]Gly-Sar uptake from the apical side in the parental Caco-2 cells (*P*) and in the nine cell lines (*clones 1–9*) cloned from Caco-2 cells. **a** The cell monolayers were incubated at 37°C for 15 min with an incubation medium containing 20 μM [^{14}C]Gly-Sar (pH 6.0) in the absence (*open column*) or in the presence (*hatched column*) of 10 mM unlabeled Gly-Sar. After washing, the radioactivity of dissolved cells was measured. **b** The specific uptake of PEPT1 was calculated by subtracting the uptake in the presence of 10 mM Gly-Sar from that in its absence. Each column represents the mean ± SE of six independent monolayers from two separate experiments. *P<0.05, significantly different from the parental Caco-2 cells

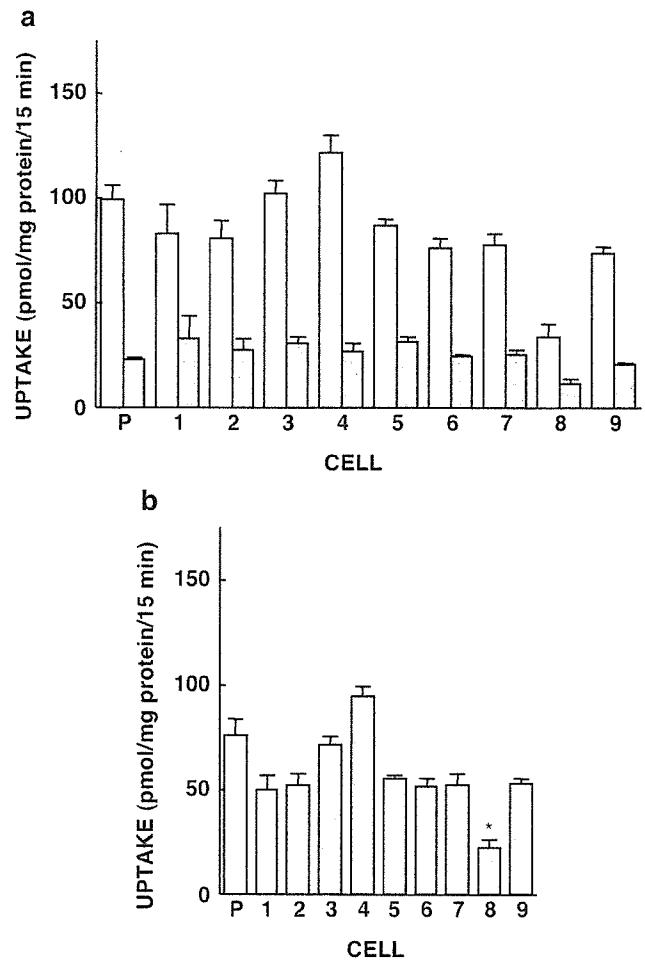

Fig. 2 [^{14}C]Gly-Sar uptake from the basolateral side in the parental Caco-2 cells (*P*) and in the nine cell lines (*clones 1–9*) cloned from Caco-2 cells. **a** The cell monolayers were incubated at 37°C for 15 min with the incubation medium containing 20 μM [^{14}C]Gly-Sar (pH 6.0) in the absence (*open column*) or in the presence (*hatched column*) of 10 mM unlabeled Gly-Sar. After washing, the radioactivity of dissolved cells was measured. **b** The specific uptake of PEPT1 was calculated by subtracting the uptake in the presence of 10 mM Gly-Sar from that in its absence. Each column represents the mean ± SE of six independent monolayers from two separate experiments. *P<0.05, significantly different from the parental Caco-2 cells

Cell culture and recloning of Caco-2 cells

Caco-2 cells at passage 18, obtained from the American Type Culture Collection (ATCC HTB37), were maintained by serial passage in plastic culture dishes, as described previously [12]. To measure the uptake of [^{14}C]Gly-Sar from the apical or basolateral side, Caco-2 cells were seeded on 12-well cluster plates (1×10^4 cells/well, 1 ml of culture medium) or on microporous membrane filters (3.0-μm pores, 1 cm^2) inside Transwell cell culture chambers (Costar, Cambridge, MA, USA) at a cell density of 6.6×10^4 cells/filter, respectively. Each Transwell chamber was filled with 0.33 and 1 ml of culture medium in the apical and basolateral compartments, respectively. For transepithelial transport studies, Caco-2 cells were seeded on microporous membrane filters (3.0-μm pores, 4.7 cm^2) at a density of 3×10^5 cells/filter and cultured with 1.5 and 2.6 ml of culture medium on the apical and basolateral sides, respectively. To prepare total RNA from the cells, Caco-2 cells were seeded on 35-mm plastic dishes (2×10^4 cells/dish, 2 ml of culture medium). Cell monolayers were given a fresh culture medium every 2–4 days and were used on the 14th or 15th day for experiments.

To obtain cell lines with different expression levels of PEPT1, parental Caco-2 cells at passage 38 were seeded on 100-mm plastic dishes at a density of 1×10^2 cells/dish. Between 3 and 4 weeks, single colonies appeared and nine colonies were picked up for subsequent experiments. In the present study, parental and cloned Caco-2 cells were used between passages 41 and 48.

Uptake and transport studies with cell monolayers

The uptake of [^{14}C]Gly-Sar from the apical or basolateral side was determined and transport studies were performed as described previously [21, 24]. Briefly, Caco-2 cells were preincubated with 2 ml of the incubation medium (pH 7.4) on both the apical and the basolateral sides for 10 min, and then 2 ml of 20 μM [^{14}C]Gly-Sar, including 0.5 μCi/ml [^{3}H]mannitol (pH 6.0) or the incubation medium (pH 7.4), was added to the apical or basolateral side, respectively. After incubation for the indicated period at 37°C, accumulation and transepithelial transport of [^{14}C]Gly-Sar and [^{3}H]mannitol were determined by liquid scintillation counting.

Quantification of PEPT1 mRNA expression

The expression levels of PEPT1 mRNA were determined by real-time polymerase chain reaction (PCR), as described previously [16]. Briefly, aliquots of 0.5 μg of total RNA, isolated from original Caco-2 cells and from each clone using the RNeasy Mini Kit (Qiagen, Hilden, Germany), were reverse-transcribed in 20 μl of reaction mixture. Real-time PCR was performed in a total volume of 20 μl containing 0.05 μg of cDNA, 1 μM forward and reverse primers, 0.2 μM TaqMan probe, and 10 μl of TaqMan Universal PCR Master Mix (Applied Biosystems, Foster City, CA, USA) under the following conditions: 50 cycles of 94°C for 15 s and 60°C for 60 s. The primer/probe set for the specific amplification of PEPT1 (accession no. NM_005703) was designed according to parameters incorporated in the Primer Express software (PE Biosystems, Foster City, CA, USA). The forward and reverse primers were ATTGTGTCGCTCTCCATTGTCTAC (positions 306–329) and ATGACCTCACAGACCACAACCAT (positions 389–367), respectively. The sequence of TaqMan probe was TTGGACAAGCAGTCACCTCAGTAAGCT CCA, corresponding to positions 334–363.

Data analysis

Each experimental point represents the mean ± SE of three to nine measurements from one to three separate experiments. Data from uptake studies were analyzed statistically by one-way analysis of variance followed by Sheffé's test. Kinetic parameters of isolated clones were statistically compared with those of parental cells by nonpaired *t* test.

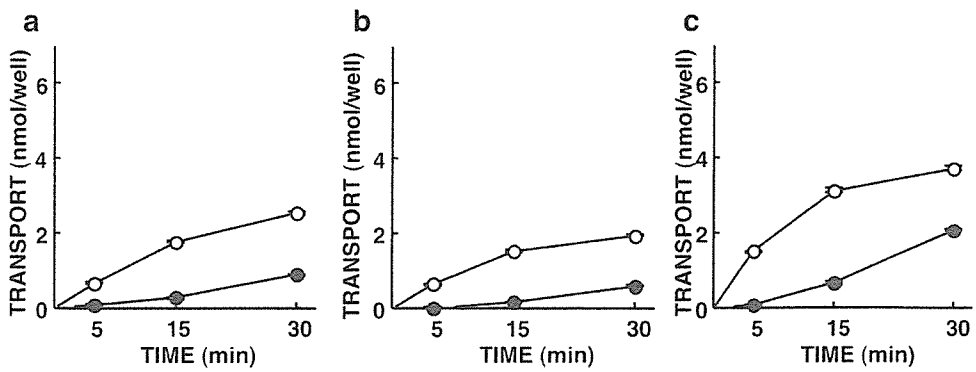

Fig. 3 [^{14}C]Gly-Sar transport from the apical side in the parental Caco-2 cells (**a**), in clone 1 (**b**), and in clone 9 (**c**). After preincubation, the cell monolayers were incubated at 37°C with 20 μM [^{14}C]Gly-Sar (pH 6.0) containing [^{3}H]mannitol, and the incubation medium (pH 7.4) was added to the apical and basolateral sides, respectively. At the indicated time, the accumulation (*circle*) and the transepithelial transport (*filled circle*) of [^{14}C]Gly-Sar were determined. The radioactivity of [^{3}H]mannitol was measured simultaneously for validation of paracellular flux (not shown). Each *symbol* represents the mean ± SE of three independent monolayers. When *error bars* are not shown, they are smaller than the *symbols*

Results

[^{14}C]Gly-Sar uptake from apical and basolateral sides in parental Caco-2 cells and in nine clones obtained by recloning of Caco-2 cells

It has been reported that Caco-2 cells, which are a useful model of intestinal epithelial cells, are heterogeneous [28]. Therefore, recloning of the parental Caco-2 cells was performed to obtain a series of cell lines differing in the expression level of PEPT1; nine clones were isolated. Compared with the parental Caco-2 cells, [^{14}C]Gly-Sar uptake from the apical side in clone 1 was markedly lower, whereas that in clone 9 was about twofold (Fig. 1). The other seven clones exhibited activity for the uptake of [^{14}C]Gly-Sar comparable to that of the parental Caco-2 cells. On the other hand, [^{14}C]Gly-Sar uptake from the basolateral side in all the clones except clone 8 did not differ significantly from that in the parental Caco-2 cells: clone 8 cells exhibited less activity (Fig. 2).

Transepithelial transport of [^{14}C]Gly-Sar in parental Caco-2 cells and in clones 1 and 9

Uptake studies suggested that two clones (clones 1 and 9) may be useful for the assessment of the transepithelial transport of Gly-Sar because the expression level of PEPT1 in each clone is different from that in the parental Caco-2 cells and because the activities of the basolateral peptide transporter in these cells are comparable. We then examined Gly-Sar transport in the absorptive direction of these cells. As shown in Fig. 3, the transepithelial transport and the accumulation of [^{14}C]Gly-Sar in clones 1 and 9 were less and greater than those in the Caco-2 cells, respectively. On the other hand, permeation of [^{3}H]mannitol, which is an index of paracellular flux, did not differ in these cells (data not shown). Results demonstrated that the intensity of PEPT1 activity obviously affects not only the accumulation but also the transepithelial transport of substrates.

Table 1 Michaelis–Menten constant (K_m) and the maximal velocity (V_{max}) of [^{14}C]Gly-Sar uptake by PEPT1 in the parental Caco-2 cells, in clone 1, and in clone 9

Cell line	Kinetic parameters	
	K_m (mM)	V_{max} (nmol/mg protein per 15 min)
Parental Caco-2	1.04±0.08	14.2±0.23
Clone 1	0.93±0.15	10.3±0.43*
Clone 9	0.98±0.11	33.0±2.64*

[^{14}C]Gly-Sar uptake from the apical side in each cell line was measured at various concentrations for 15 min, and then the kinetic parameters were determined by nonlinear least squares regression analysis according to the Michaelis–Menten equation. Each value represents the mean ± SE of three independent experiments
*P<0.05, significantly different from the value of the parental cells

Kinetic analysis of [^{14}C]Gly-Sar uptake by PEPT1

Next, we performed a kinetic analysis of [^{14}C]Gly-Sar uptake from the apical side in the parental cells and in clones 1 and 9. As illustrated in Fig. 4, [^{14}C]Gly-Sar uptake in these cells was saturable, and kinetic parameters were estimated according to the Michaelis–Menten equation using nonlinear least squares regression analysis. As summarized in Table 1, the maximal velocity (V_{max}) of [^{14}C]Gly-Sar uptake in clones 1 and 9 was significantly lower and greater than that in the parental Caco-2 cells, respectively. However, Michaelis–Menten constants (K_m) were comparable among these cells. These findings suggested that the differences in the activities of [^{14}C]Gly-Sar uptake among the three cell lines are caused by the different expression levels of PEPT1 protein.

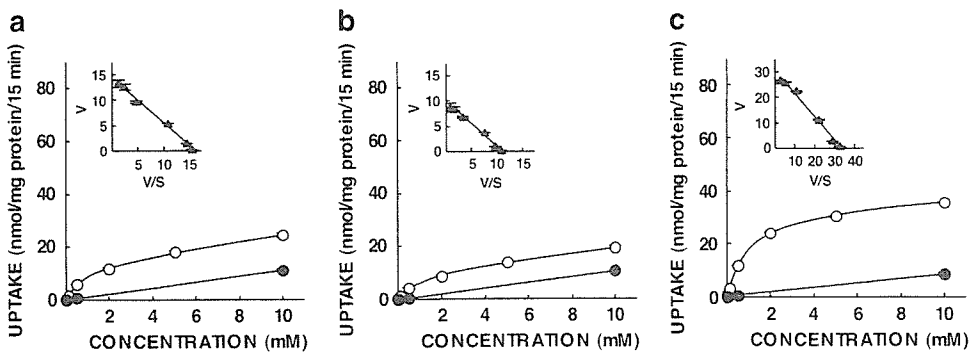

Fig. 4 Concentration dependence of [^{14}C]Gly-Sar uptake from the apical side in the parental Caco-2 cells (**a**), in clone 1 (**b**), and in clone 9 (**c**). [^{14}C]Gly-Sar uptake was measured at various concentrations for 15 min in the absence (*circle*) or in the presence (*filled circle*) of 50 mM glycyl-leucine. These figures show the representative data of three experiments. Each *point* represents the mean ± SE of three monolayers. When *error bars* are not shown, they are smaller than the *symbols*. *Insets*: Eadie–Hofstee plots of [^{14}C]Gly-Sar uptake after correction for nonspecific component (*filled triangle*). *V* Uptake rate (nmol/mg protein per 15 min), *S* [^{14}C]Gly-Sar concentration (mM)

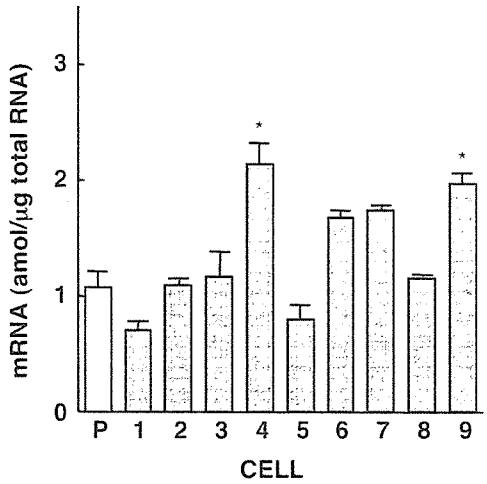

Fig. 5 Quantification of PEPT1 mRNA expressed in the parental Caco-2 cells (*P*) and in the nine cell lines (*clones1–9*). Total cellular RNA was extracted from the cells and then reverse-transcribed. The mRNA levels of PEPT1 in these cells were determined by real-time PCR using an ABI Prism 7700 sequence detector. Each column represents the mean ± SE of five to eight independent monolayers from two or three separate experiments. *P<0.05, significantly different from the parental Caco-2 cells

Expression levels of PEPT1 mRNA in parental Caco-2 cells and in isolated clones

Moreover, the amount of PEPT1 mRNA expressed in the parental Caco-2 cells and in the nine clones was determined by real-time PCR. As shown in Fig. 5, the expression level of PEPT1 mRNA in clone 1 was lower than that in the parental cells. In contrast, clone 9 displayed a level of expression that was higher than that of the parental Caco-2 cells. These findings were consistent with the activity of [^{14}C]Gly-Sar uptake from the apical side in these cells (Fig. 1). On the other hand, clone 4 exhibited a greater level of PEPT1 mRNA expression, despite activities of PEPT1 comparable to those of the parental Caco-2 cells.

To further examine whether the expression level of PEPT1 mRNA can serve as an indicator of PEPT1 activity, the correlation between the uptake of [^{14}C]Gly-Sar and the amount of PEPT1 mRNA was investigated in the parental and cloned cells at passages 41 and 46 in order to increase the number of samples. Figure 6 shows the linear regression of the activity of [^{14}C]Gly-Sar uptake from the apical side against the expression level of PEPT1 mRNA in the parental Caco-2 cells and in the nine clones. A positive linear correlation was observed with r=0.55.

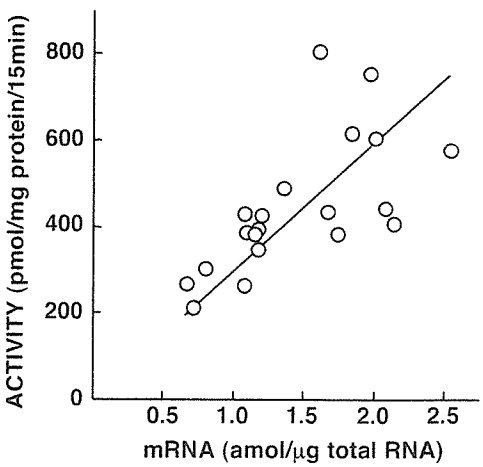

Fig. 6 The linear regression of the activity of [^{14}C]Gly-Sar uptake against the expression level of PEPT1 mRNA in the parental Caco-2 cells and in the nine clones. [^{14}C]Gly-Sar uptake was measured experimentally, and the amount of PEPT1 mRNA was determined by real-time PCR in the same batch of the respective cells. Each *symbol* was plotted using the mean of [^{14}C]Gly-Sar uptake and that of mRNA expression in three independent monolayers

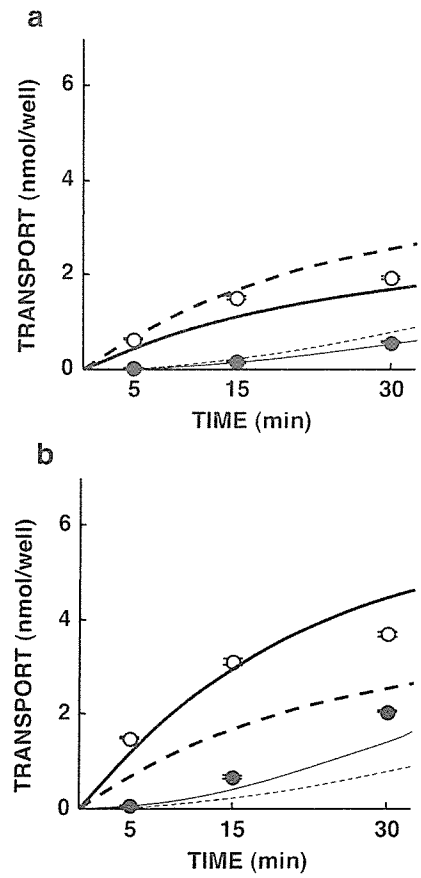

Fig. 7 Simulation of Gly-Sar transport in two clones. The accumulation and the transepithelial transport of 20 μM Gly-Sar in clone 1 (**a**) and in clone 9 (**b**) in the absorptive direction were simulated using the expanded computational model. The curves were delineated using the values of Gly-Sar transport calculated every 0.01 min with a program written in Visual Basic.NET. Numeric integration is based on Euler's method. The *bold* and *fine curves* represent the simulated accumulation and the transepithelial transport of Gly-Sar, respectively. The *solid* and *broken curves* display the simulation by the expanded and the previous models for Gly-Sar transport, respectively. The *symbols* represent the experimental data of the accumulation (*circle*) and the transepithelial transport (*filled circle*) of [^{14}C]Gly-Sar

Simulation for transepithelial transport of Gly-Sar

Based on the above findings, we chose the amount of PEPT1 mRNA as an index for the intensity of the transport activity of PEPT1. In the previous model, the maximal velocity (V_{max}) of PEPT1 in the influx direction was estimated using the parental Caco-2 cells and was defined as a constant value [11]. To incorporate mathematically the amount of PEPT1 mRNA to the simulator as a relative factor of PEPT1 activity, the V_{max} of PEPT1 in the influx direction was regarded as a variable using the following equation: $V_{max\,PEPT1.\,uptake} = 4.164 \times mRNA/1.073$ where "4.164" is the V_{max} value (nmol/min per milligram of protein) determined in the previous study [11] and "1.073" is the mean of PEPT1 mRNA (amol/μg total RNA) expressed in the parental Caco-2 cells in this study. $V_{maxPEPT1,\,uptake}$ represents the V_{max} value after correction (nmol/min per milligram of protein), and mRNA stands for the amount of mRNA (amol/μg total RNA) in the cells compared.

To validate the model, Gly-Sar transport in clones 1 and 9 was simulated using both the previous model and the improved model. The mean of the amount of PEPT1 mRNA expressed in clones 1 and 9 was 0.712 and 1.963 (amol/μg total RNA), respectively. As shown in Fig. 7, the simulation using the model developed in this study corresponded more closely with experimental data than that using the previous model, indicating that the improved model can achieve a change in the expression level of PEPT1.

Discussion

It has been proposed that computational modeling can provide a tool for the reproduction and understanding of physiological and molecular biological phenomena in which multiple factors participate [5, 9, 15, 22]. Because of the diversity and multispecificity of drug transporters, the behavior of a drug is complicated; therefore, computational modeling of drug transporters will be useful in predicting drug behavior and in studying the relationship and contribution of transporters.

Recently, based on a detailed examination of the functional properties of PEPT1 and the basolateral peptide transporter, we constructed a mathematical model of Gly-Sar transport in Caco-2 cells [11]. This model could predict Gly-Sar transport, but could not achieve a change in the expression level of PEPT1. With respect to various drug transporters including PEPT1, the expression levels of transporters were proven to affect the pharmacokinetic properties of substrates [8, 18, 20]. Furthermore, it has been demonstrated that the expression levels of PEPT1 in the small intestine differ among the segments [17] and that PEPT1 is regulated by a variety of factors [2]. Therefore, to establish a simulator of drug absorption, it is essential that the model encompasses an alteration in PEPT1 expression. To address this issue, the V_{max} value of PEPT1 is defined as a variable reflecting the expression level and is described mathematically using the amount of PEPT1 mRNA in this study. With this improved model, Gly-Sar transport in cloned cells expressing the lowest and the highest levels of PEPT1 was predicted more accurately than with the previous model (Fig. 7), indicating that our model can simulate the behavior of Gly-Sar in Caco-2 cells even if the expression level of PEPT1 is altered.

Chu et al. [4] demonstrated that PEPT1 protein expression and cephalexin uptake exhibited a good correlation using Caco-2 cells expressing PEPT1 at various levels. Furthermore, they also found that PEPT1 protein expression was well-correlated with PEPT1 mRNA level, although the data were not shown. Consistent with their report, a correlation between the transport activity and the mRNA expression of PEPT1 was confirmed in cells isolated from the parental Caco-2 cells in this study. These results suggest that the amount of PEPT1 mRNA is an appropriate index for a mathematical description of the PEPT1 expression level when a change in the activity of PEPT1 accompanies that in the PEPT1 gene expression. Besides transcriptional regulation, it has been reported that several signals, such as insulin [25] and leptin [3], induce an alteration in the PEPT1 protein expression without any change in the amount of PEPT1 mRNA. The mechanism of insulin and leptin regulation was suggested to be increased trafficking of the PEPT1 proteins from the cytoplasmic pool to the apical membranes. Because of inconvenience and difficulty, however, the determination of absolute PEPT1 protein expression level seems to be unavailable as an index of PEPT1 expression for improvement of the simulator. Therefore, we chose the expression of PEPT1 mRNA as an index and incorporated it into our model. Further studies and new technologies are needed to overcome problems in the handling of regulation that do not parallel alterations in the PEPT1 mRNA expression.

It was observed that the activity of [^{14}C]Gly-Sar uptake in clone 4 was comparable to that in the parental Caco-2 cells in spite of the higher expression of PEPT1 mRNA. In addition, more dispersion was observed in the analysis of the correlation between the activity and the mRNA expression of PEPT1 in this study compared to the previous study [4]. These differences may be caused by used cells: Chu et al. [4] used PEPT1-overexpressed Caco-2 cells established by an adenoviral transfection system, whereas we used clones isolated from the parental Caco-2 cells. It is possible that not only the expression of PEPT1 but also that of other molecules affecting the apparent activity of Gly-Sar uptake (such as Na^+/H^+ exchanger 3) [13] differ from that of the clones. Likely, several factors (other than PEPT1) among the parental cloned cells may be responsible for the slight disagreement in the simulation using the improved model with experimental data (Fig. 7). These findings suggest that, besides PEPT1, other factors should be described mathematically and incorporated into the model.

In conclusion, to adjust the previous model for the simulation of Gly-Sar transport in accordance with a change in the expression level of PEPT1, the V_{max} value of PEPT1 in the influx direction was defined mathematically using the

amount of PEPT1 mRNA as an index of the PEPT1 expression level. The improved model could well reproduce the transport of Gly-Sar in the cells expressing PEPT1 at the highest and the lowest levels. These findings suggest that our model can predict Gly-Sar transport even when PEPT1 is expressed at a different level and that the developed model may underlie a simulator for the prediction of drug absorption in the small intestine.

Acknowledgements This work was supported, in part, by the Leading Project for Biosimulation, the 21st Century COE Program "Knowledge Information Infrastructure for Genome Science," and a Grant-in-Aid for Scientific Research from the Ministry of Education, Culture, Sports, Science, and Technology of Japan. Megumi Irie is a Research Fellow of the Japan Society for the Promotion of Science.

References

1. Adibi SA (1997) The oligopeptide transporter (Pept-1) in human intestine: biology and function. Gastroenterology 113:332–340
2. Adibi SA (2003) Regulation of expression of the intestinal oligopeptide transporter (Pept-1) in health and disease. Am J Physiol Gastrointest Liver Physiol 285:G779–G788
3. Buyse M, Berlioz F, Guilmeau S, Tsocas A, Voisin T, Péranzi G, Merlin D, Laburthe M, Lewin MJM, Rozé C, Bado A (2001) PepT1-mediated epithelial transport of dipeptides and cephalexin enhanced by luminal leptin in the small intestine. J Clin Invest 108:1483–1494
4. Chu X-Y, Sánchez-Castaño GP, Higaki K, Oh D-M, Hsu C-P, Amidon GL (2001) Correlation between epithelial cell permeability of cephalexin and expression of intestinal oligopeptide transporter. J Pharmacol Exp Ther 299:575–582
5. Clancy CE, Rudy Y (1999) Linking a genetic defect to its cellular phenotype in a cardiac arrhythmia. Nature 400:566–569
6. Daniel H (2004) Molecular and integrative physiology of intestinal peptide transport. Annu Rev Physiol 66:361–384
7. Daniel H, Kottra G (2004) The proton oligopeptide cotransporter family SLC15 in physiology and pharmacology. Pflugers Arch 447:610–618
8. Hashida T, Masuda S, Uemoto S, Saito H, Tanaka K, Inui K (2002) Pharmacokinetic and prognostic significance of intestinal MDR1 expression in recipients of liver-donor liver transplantation. Clin Pharmacol Ther 69:308–316
9. Hoffmann A, Levchenko A, Scott ML, Baltimore D (2002) The IκB–NF-κB signaling module: temporal control and selective gene activation. Science 298:1241–1245
10. Inui K, Yamamoto M, Saito H (1992) Transepithelial transport of oral cephalosporins by monolayers of intestinal epithelial cell line Caco-2: specific transport systems in apical and basolateral membranes. J Pharmacol Exp Ther 261:195–201
11. Irie M, Terada T, Okuda M, Inui K (2004) Efflux properties of basolateral peptide transporter in human intestinal cell line Caco-2. Pflugers Arch 449:186–194
12. Irie M, Terada T, Sawada K, Saito H, Inui K (2001) Recognition and transport characteristics of nonpeptidic compounds by basolateral peptide transporter in Caco-2 cells. J Pharmacol Exp Ther 298:711–717
13. Kennedy DJ, Leibach FH, Ganapathy V, Thwaites DT (2002) Optimal absorptive transport of the dipeptide glycylsarcosine is dependent on functional Na^+/H^+ exchange activity. Pflugers Arch 445:139–146
14. Leibach FH, Ganapathy V (1996) Peptide transporters in the intestine and the kidney. Annu Rev Nutr 16:99–119
15. Matsuoka S, Sarai N, Kuratomi S, Ono K, Noma A (2003) Role of individual ionic current systems in ventricular cells hypothesized by a model study. Jpn J Physiol 53:105–123
16. Motohashi H, Sakurai Y, Saito H, Masuda S, Urakami Y, Goto M, Fukatsu A, Ogawa O, Inui K (2002) Gene expression levels and immunolocalization of organic ion transporters in the human kidney. J Am Soc Nephrol 13:866–874
17. Naruhashi K, Sai Y, Tamai I, Suzuki N, Tsuji A (2002) Pept1 mRNA expression is induced by starvation and its level correlates with absorptive transport of cefadroxil longitudinally in the rat intestine. Pharm Res 19:1417–1423
18. Pan X, Terada T, Irie M, Saito H, Inui K (2002) Diurnal rhythm of H^+-peptide cotransporter in rat small intestine. Am J Physiol Gastrointest Liver Physiol 283:G57–G64
19. Saito H, Inui K (1993) Dipeptide transporters in apical and basolateral membranes of the human intestinal cell line Caco-2. Am J Physiol Gastrointest Liver Physiol 265:G289–G294
20. Sakurai Y, Motohashi H, Ueo H, Masuda S, Saito H, Okuda M, Mori N, Matsuura M, Doi T, Fukatsu A, Ogawa O, Inui K (2004) Expression levels of renal organic anion transporters (OATs) and their correlation with anionic drug excretion in patients with renal diseases. Pharm Res 21:61–67
21. Sawada K, Terada T, Saito H, Inui K (2001) Distinct transport characteristics of basolateral peptide transporters between MDCK and Caco-2 cells. Pflugers Arch 443:31–37
22. Schoeberl B, Eichler-Jonsson C, Gilles ED, Müller G (2002) Computational modeling of the dynamics of the MAP kinase cascade activated by surface and internalized EGF receptors. Nat Biotechnol 20:370–375
23. Terada T, Inui K (2004) Peptide transporters: structure, function, regulation and application for drug delivery. Curr Drug Metab 5:85–94
24. Terada T, Sawada K, Saito H, Inui K (1999) Functional characteristics of basolateral peptide transporter in the human intestinal cell line Caco-2. Am J Physiol Gastrointest Liver Physiol 276:G1435–G1441
25. Thamotharan M, Bawani SZ, Zhou X, Adibi SA (1999) Hormonal regulation of oligopeptide transporter Pept-1 in a human intestinal cell line. Am J Physiol Cell Physiol 276: C821–C826
26. Thwaites DT, Brown CDA, Hirst BH, Simmons NL (1993) Transepithelial glycylsarcosine transport in intestinal Caco-2 cells mediated by expression of H^+-coupled carriers at both apical and basal membranes. J Biol Chem 268:7640–7642
27. Thwaites DT, Brown CDA, Hirst BH, Simmons NL (1993) H^+-coupled dipeptide (glycylsarcosine) transport across apical and basal borders of human intestinal Caco-2 cell monolayers display distinctive characteristics. Biochim Biophys Acta 1151:237–245
28. Vachon PH, Beaulieu J-F (1992) Transient mosaic patterns of morphological and functional differentiation in the Caco-2 cell line. Gastroenterology 103:414–423
29. Yang CY, Dantzig AH, Pidgeon C (1999) Intestinal peptide transport systems and oral drug availability. Pharm Res 16:1331–1343

Pharmaceutical Research, Vol. 23, No. 4, April 2006 (© 2006)
DOI: 10.1007/s11095-006-9665-2

Research Paper

Androgen Receptor is Responsible for Rat Organic Cation Transporter 2 Gene Regulation but not for rOCT1 and rOCT3

Jun-ichi Asaka,[1] Tomohiro Terada,[1] Masahiro Okuda,[1] Toshiya Katsura,[1] and Ken-ichi Inui[1,2]

Received October 18, 2005; accepted December 7, 2005

Purpose. Organic cation transporters 1–3 (OCT1–3; Slc22a1–3) mediate the membrane transport of organic cations in the kidney. We previously reported that rat (r)OCT2 expression in the kidney was regulated by testosterone. In this study, we examined the transcriptional mechanisms underlying the testosterone-dependent regulation of rOCT2 expression.
Methods. Approximately 3000-bp fragments of the rOCT1–3 promoter region were isolated, and promoter activities were measured in the renal epithelial cell line LLC-PK_1 with the coexpression of rat androgen receptor.
Results. Among reporter constructs tested, only rOCT2 promoter activity was stimulated by testosterone. This stimulation was suppressed by nilutamide, an antiandrogen drug. Reporter assays using deletion constructs and mutational constructs of putative androgen response elements (ARE) in the rOCT2 promoter region suggested that two AREs, located at approximately −3000 and −1300, respectively, play an important role in the induction by testosterone.
Conclusions. Testosterone induces the expression of rOCT2, but not of rOCT1 and rOCT3, via the AR-mediated transcriptional pathway. This is the first study to address the transcriptional mechanisms of testosterone-dependent gene regulation of the Slc22 family.

KEY WORDS: gender difference; kidney; promoter; rOCT2; testosterone.

INTRODUCTION

Proximal tubules play important roles in the renal elimination of drugs. Cationic drugs are secreted from blood to urine by combined efforts of two distinct classes of organic cation transporters: one driven by the transmembrane electrical potential difference in the basolateral membranes, and the other driven by the transmembrane H^+ gradient in the brush-border membranes (1). Molecular cloning studies identified three kinds of organic cation transporters (OCT1–3), and their physiological and pharmacokinetic roles have been evaluated (2,3). Rat (r)OCT1 (Slc22a1) is expressed abundantly in the liver and kidney (4), whereas rOCT2 (Slc22a2) is expressed in the kidney, but not in the liver (5). These transporters are localized to the basolateral membranes of renal proximal tubules (6,7). rOCT3 (Slc22a3) is expressed predominantly in the placenta, and also in the intestine, heart, brain, lung, and very weakly in the kidney (8). Functional studies using heterologous expression systems revealed that all OCTs recognized a variety of organic cations with different molecular structures including tetraethylammonium, 1-methyl-4-phenylpyridinium, N^1-methylnicotinamide, choline, and dopamine (8,9).

It was reported that the uptake of tetraethylammonium was greater in renal cortical slices of male rats than female rats (10), suggesting gender differences in the basolateral membrane transport activity for organic cations. We found that expression level of rOCT2, but neither rOCT1 nor rOCT3, in the kidney was much higher in males than females and suggested that rOCT2 is responsible for gender differences in renal basolateral membrane organic cation transport activity (11). Furthermore, we demonstrated that treatment of male and female rats with testosterone significantly increased rOCT2 expression in the kidney (12). These results suggested that testosterone plays a pivotal role in the transcriptional regulation of the rOCT2 gene. However, no information has been available to demonstrate this process.

Androgens, such as testosterone, are main hormones responsible for the male phenotype (13). As with other steroid hormones, many effects of androgen are mediated by a specific intracellular androgen receptor (AR; NR3C4). AR activated by testosterone binds to the androgen response element (ARE) in the 5′-flanking region of target genes and is responsible for the expression of various genes such as the C3 subunit of prostatin (14) and prostate-specific antigen gene (15). Based on our previous studies, we hypothesized that AR could be involved in the regulation of the rOCT2 gene.

[1] Department of Pharmacy, Kyoto University Hospital, Faculty of Medicine, Kyoto University, Sakyo-ku, Kyoto 606-8507, Japan.
[2] To whom correspondence should be addressed. (e-mail: inui@kuhp.kyoto-u.ac.jp)

ABBREVIATIONS: AR, androgen receptor; ARE, androgen response element; bp, base pair; CYP, cytochrome P450; DMEM, Dulbecco's modified Eagle's medium; FBS, fetal bovine serum; MMTV, mouse mammary tumor virus; OCT, organic cation transporter; PCR, polymerase chain reaction; RACE, rapid amplification of cDNA ends.

In the present study, therefore, we examined the effects of testosterone on the promoter activities of rOCTs to understand the role of this hormone in the gender differences of rOCT2 expression.

MATERIALS AND METHODS

Materials

Restriction enzymes were obtained from New England BioLabs (Beverly, MA, USA). T4 kinase and T4 DNA ligase were purchased from TaKaRa (Ootu, Japan). [α-^{32}P] CTP was obtained from Amersham Biosciences, Inc. (Buckinghamshire, UK). Testosterone was purchased from Nacalai Tesque (Kyoto, Japan). Nilutamide was obtained from Sigma (St. Louis, MO, USA).

Determination of Putative Transcriptional Start Sites

The putative transcriptional start sites for rOCT1-3 were determined by 5′-rapid amplification of cDNA ends (5′-RACE) using the rat Marathon-Ready cDNA kit (Clontech, Palo Alto, CA, USA) according to the manufacturer's instructions. The rOCT2 gene-specific primers for the 5′-RACE were designed and synthesized based on the genomic sequence. The 5′-RACE was performed with adapter primer 1 that came with the kit and a gene-specific primer of rOCT1 (accession number NM_012697), 5′-CACAACCAGGGAGCCCAGGAAGAAG CCC-3′ (538 to 511). Nested polymerase chain reaction (PCR) was performed with adapter primer 2 and a nested gene-specific primer of rOCT1, 5′-CAGGAAGGCTTGTTTCTGGAAC CAGCCA-3′ (106 to 79). The rOCT2 gene-specific primers are as follows: a gene-specific primer of rOCT2 (accession number NM_031584), 5′-CCTTCATAAGAGGTTGTTAA GCCTGCCACTGGA-3′ (605 to 577); a nested gene-specific primer of rOCT2, 5′-GGAGGCACCAGACAGCAGGCT AAGAGG-3′ (187 to 160). The rOCT3 gene-specific primers are as follows: a gene-specific primer of rOCT3 (accession number NM_019230), 5′-GCCCAGGAAGACCACACCAA CGAAGAG-3′ (520 to 493); a nested gene-specific primer of rOCT3, 5′-GTCAGGCACAGCAGCAGGAACACGCG CC-3′ (474 to 450).

Genomic Cloning of rOCT1, rOCT2, and rOCT3 Promoters

rOCT1 and rOCT3 promoters were isolated from the rat genome (Clontech) by a PCR-based method using the following primers designed based on the rat genomic DNA (accession number AC114389): rOCT1 sense 5′-GGACGCGTCCA TGCTCTGCGAACTGAGGT-3′ and antisense 5′-GGCTC GAGGACTGCCACCAGGGGTTCAT-3′; rOCT3 sense 5′-GGACGCGTCCCTTCGAAGCAGAGGGAAAA-3′ and antisense 5′-GGAGATCTTGCAGGAATAGCCTCCAGT GC-3′. On the other hand, the rOCT2 promoter was isolated from the rat genomic library (Clontech) with a conventional plaque hybridization method. The probe was prepared by PCR using rat genomic DNA (Clontech) as a template. The primers, designed based on the rat genomic DNA (accession number AC114389), were as follows: 5′-GGCTTGGGAGAT GGCTAAGTA-3′ and 5′-TCACAGCCATGTGGGACA TGT-3′. Phage DNA with a long rOCT2 promoter was prepared with a QIAGEN lambda midi kit (Qiagen, Hilden, Germany) and partially sequenced. The transcription factor-binding sites were predicted with TRANSFAC 5.0 software (http://www.gene-regulation.com/cgi-bin/pub/programs/match/bin/match.cgi?), with a core similarity of 0.95 and a matrix similarity of 0.90.

Construction of Reporter Gene and Rat Androgen Receptor Expression Plasmid

Approximately 3-kb fragments corresponding to the 5′-flanking regions of the rOCT genes were subcloned into a pGL3-Basic luciferase gene vector (Promega, Madison, WI, USA) to yield rOCT1 (−3025/+23), rOCT2 (−3036/+242), and rOCT3 (−3001/+31). The deletion constructs rOCT2 (−1895/+242), rOCT2 (−819/+242), rOCT3 (−1095/+31), and rOCT3 (−515/+31) were prepared with the restriction enzymes. The mouse mammary tumor virus (MMTV) gene excised from pMSG (Amersham Biosciences) was subcloned into pGL3 to yield MMTV-pGL3.

ARE mutants were constructed using QuikChange® II Site-Directed Mutagenesis Kit (Stratagene, La Jolla, CA, USA) according to the manufacturer's instructions. Primer sequences are listed in Table I.

Table I. Sequences of Mutation Primers

Primer	Sequence
ARE-1 S	5′-GGCCTCTGTGGTAGAGGA**GCC**ACTTAATCTTGCTGC-3′
ARE-1 AS	5′-GCAGCAAGATTAAGTGGCTCCTCTACCACAGAGGCC-3′
ARE-2 S	5′-CCTATGAGGACCAAGC**GCC**ACTCTCATGTCCTTCCTG-3′
ARE-2 AS	5′-CAGGAAGGACATGAGAGTGGCGCTTGGTCCTCATAGG-3′
ARE-3 S	5′-CCTTGGCACAGGA**GCC**TCTCCTTGACTCTCACCTG-3′
ARE-3 AS	5′-CAGGTGAGAGTCAAGGAGAGGCTCCTGTGCCAAGG-3′
ARE-4 S	5′-GCGTCCTGATACAGAC**GCC**ACCCATGAGTCAGTCAC-3′
ARE-4 AS	5′-GTGACTGACTCATGGGTGGCGTCTGTATCAGGACGC-3′
ARE-5 S	5′-CAGCAGGAAAGAGAGACTACC**GCC**TTCCCTGGCATTTGG-3′
ARE-5 AS	5′-CCAAATGCCAGGGAAGGCGGTAGTCTCTCTTTCCTGCTG-3′

Underlined sequences are putative ARE sequences, and bold characters indicate positions of the ARE mutation.
ARE = androgen response element.

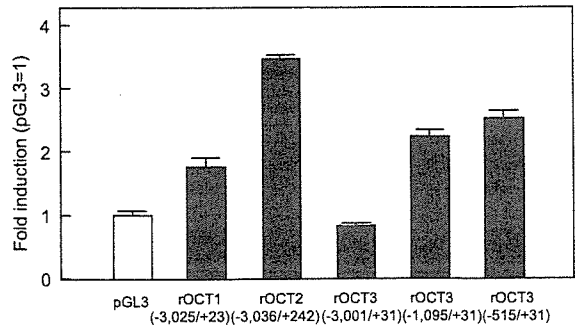

Fig. 1. Promoter activities of rat organic cation transporter (rOCT) genes. rOCT1–3 promoter constructs were transfected into LLC-PK_1 cells for luciferase assays. Firefly luciferase activity was normalized to *Renilla* luciferase activity. Each column represents the mean ± SE of three independent experiments.

cDNA for rat AR (rAR: accession number, NM_012502) was isolated from rat kidney cDNA by a PCR-based method using the following primers: sense 5′-GGGATCCAGGATG GAGGTGCAGTTAGGG-3′ (991 to 1011) and antisense 5′-GGCTCGAGTTTCCAAATCTTCACTGTGTG-3′ (3713 to 3693). PCR was performed using Pfu polymerase (Stratagene) as follows: 95°C for 3 min; 35 cycles of 95°C for 1 min, 60°C for 1 min, 72°C for 8 min; and a final extension at 72°C for 10 min. The PCR product was subcloned into the expression vector pBK-CMV (Stratagene).

Cell Culture and Luciferase Assay

The porcine kidney epithelial cell line LLC-PK_1 was obtained from American Type Culture Collection (ATCC CRL-1392; Rockville, MD) and cultured as described previously (16). For the luciferase assay, the cells were seeded at 1.5×10^5 cells into 24-well plates in Dulbecco's modified Eagle's medium (DMEM), supplemented with 10% charcoal-stripped fetal bovine serum (FBS). Cells were transfected by 5-h exposure to LipofectAMINEplus (Invitrogen Japan KK, Tokyo, Japan), with each well containing 0.6 μg of the rOCT2 (−3036/+242) or equimolar amount of other reporter constructs, 0.1 μg of the rAR expression vector, and 30 ng of an internal control vector for transfection efficiency, namely, the *Renilla* luciferase (pRL-TK) reporter plasmid (Promega) in serum-free DMEM. The medium was changed to DMEM supplemented with 10% charcoal-stripped FBS, containing testosterone, nilutamide, or the vehicle control, dimethyl sulfoxide. After 43-h incubation, the cells were harvested and lysed, and luciferase activity was determined using a dual luciferase assay kit (Promega) and a LB940 luminometer (Berthold, Bad Wildbad, Germany). Each reporter construct was assayed in triplicate wells, and each experiment was repeated three times.

Statistical Analysis

The data were expressed as the mean ± SE. The significance of differences between the vehicle-treated and testosterone-treated groups was analyzed using Dunnet's *post hoc* analysis. Other analyses were conducted with Student's *t* test. Significance was set at $p < 0.05$.

RESULTS

Determination of the Transcriptional Start Site(s) for rOCTs in Rat Kidney Using 5′-RACE

The transcriptional start site(s) for rOCTs in the rat kidney were identified using 5′-RACE. The putative transcriptional start sites were determined using the longest RACE product. Sequencing of the amplified bands revealed that the terminal position of rOCT1 cDNA with the longest 5′-untranslated region was located 63 nucleotides above the start codon, which is 26 bp upstream of the 5′-end of rOCT1 cDNA reported previously (4). The terminal position of rOCT2 cDNA was located 306 nucleotides above the start codon, which is 266 bp upstream of the 5′-end of rOCT2 cDNA (5). The terminal position of rOCT3 cDNA is 35 nucleotides above the start codon, which is 359 bp downstream of the 5′-end of rOCT3 cDNA (8). Therefore, the terminal position of

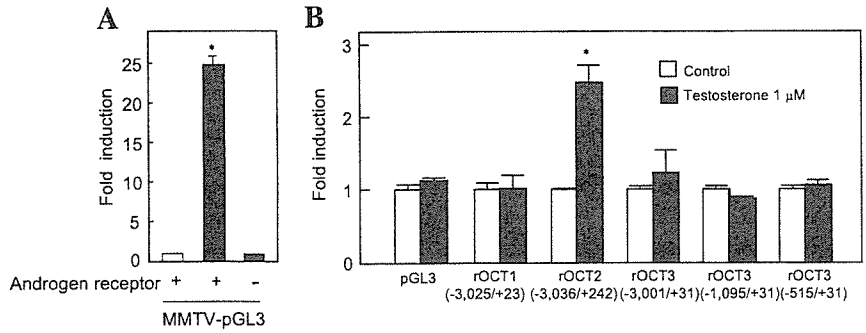

Fig. 2. (A) *Trans*-activation of the mouse mammary tumor virus (MMTV) promoter by rat androgen receptor (rAR) in the presence of testosterone. (B) *Trans*-activation of rOCT1–3 promoters by rAR in the presence of testosterone. Constructs were transiently transfected into LLC-PK_1 cells with rAR and pRL-TK. The cells were cultured for 43 h with vehicle or 1 μM testosterone, and luciferase activity was measured. Firefly luciferase activity was normalized to *Renilla* luciferase activity. Each column represents the mean ± SE of three independent experiments. *$p < 0.05$, significantly different from control.

rOCT cDNA with the longest 5′-untranslated region was numbered with +1 as the transcription start site in this study.

Isolation and Analysis of 5′-Flanking Region of rOCT Genes

Based on the transcriptional start site, we then isolated the promoter region (about 3 kb) of each transporter and prepared reporter constructs. For luciferase assay, we used LLC-PK_1 cells because LLC-PK_1 cells possessed organic cation transport activities (16,17) and pig organic cation transporter OCT2p (18). Figure 1 shows the basal promoter activities of each transporter in LLC-PK_1 cells. Reporter constructs for rOCT1 and rOCT2 showed significant promoter activity. A reporter construct for rOCT3 (−3001/+31) did not have promoter activity, but those for rOCT3 (−1095/+31) and rOCT3 (−505/+31) did, suggesting that a repressive region is located in the rOCT3 promoter region −3001 to −1095. These findings suggest that all promoter constructs function appropriately.

Using these constructs, the effects of testosterone on the promoter activities were assessed. The functional activity of rAR was confirmed by a reporter assay using MMTV reporter construct in the presence of 1 μM testosterone (Fig. 2A). AR has been shown to *trans*-activate MMTV promoter using testosterone (19). In the absence of rAR, MMTV promoter activity was not enhanced by testosterone; native AR was not expressed in LLC-PK_1 cells. As shown in Fig. 2B, the activity of the rOCT2 promoter was significantly enhanced by testosterone, but that of the rOCT1 and rOCT3 promoters was not. These results were consistent with our previous results of Northern blotting (11). We therefore further characterized the transcriptional mechanisms by which the rOCT2 promoter is stimulated by testosterone.

Figure 3 shows the nucleotide sequence for 1000 bp upstream of the translation start site of the rOCT2 gene. Putative binding sites for many transcription factors were identified by TRANSFAC with a core similarity of 0.95 and a matrix similarity of 0.90, including activating protein (AP)-1, octamer-binding factor (Oct)-1, HNF-3/Fkh Homolog (HFH)-3, and a CCAAT box.

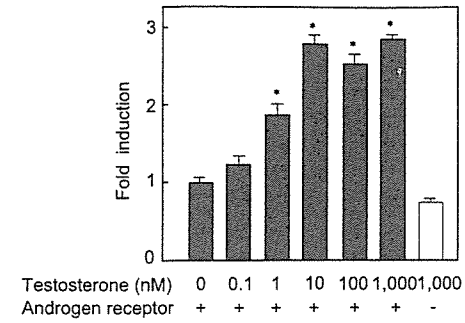

Fig. 4. *Trans*-activation of the rOCT2 promoter (−3036/+242) by rAR in the presence of testosterone. Constructs were transiently transfected into LLC-PK_1 cells with rAR and pRL-TK. The cells were cultured in the presence or absence of testosterone for 43 h. The vector pBK-CMV was used instead of rAR, and luciferase activity was measured. Firefly luciferase activity was normalized to *Renilla* luciferase activity. Each column represents the mean ± SE of three independent experiments. $*p < 0.05$, significantly different from 0 nM testosterone.

Region of 5′-Flanking Sequence Required for Response to Testosterone

As shown in Fig. 4, a reporter construct for rOCT2 (−3036/+242) was significantly activated by testosterone in a concentration-dependent manner, and about a 3-fold increase was observed with 10 nM testosterone. Testosterone did not activate the rOCT2 promoter construct in the absence of the rAR expression vector. Nilutamide, an antiandrogen drug, acts as a competitive inhibitor of the androgen receptor (20). Nilutamide blocked the activation of the rOCT2 promoter by testosterone in a dose-dependent manner (Fig. 5), but nilutamide is a partial agonist of androgen receptor; rOCT2 activity is not completely suppressed by nilutamide. These findings suggest that rOCT2 promoter activity is stimulated by AR. Therefore, we tried to identify ARE(s) that work to stimulate rOCT2 promoter activity.

Table II shows sequences, positions, and homology to the consensus sequence of ARE within the 3000 bp of rOCT2

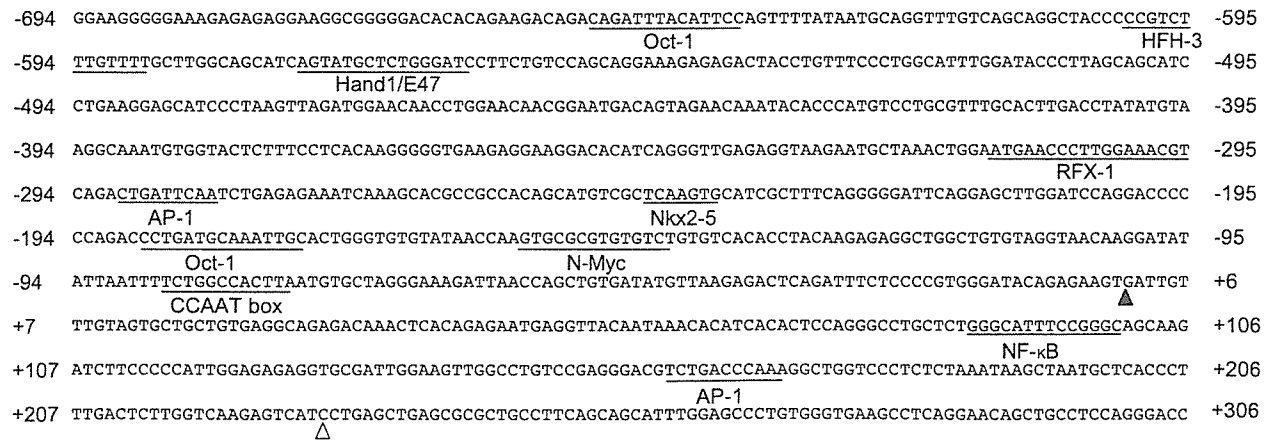

Fig. 3. Transcriptional elements of the rOCT2 promoter. A 1000-base genomic DNA sequence immediately upstream of the start codon site is listed. An open triangle indicates the putative transcriptional start position, and a closed triangle indicates the 5′-end of rOCT2 cDNA published so far (NM_031584).

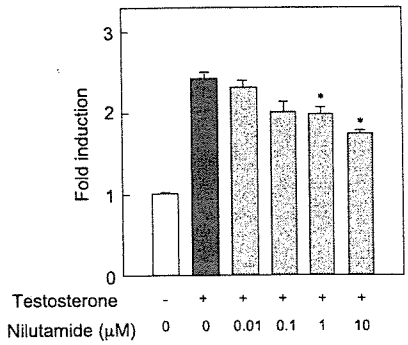

Fig. 5. The effect of nilutamide on *trans*-activation of the rOCT2 promoter (−3036/+242) by rAR in the presence of testosterone. Constructs were transiently transfected into LLC-PK$_1$ cells with rAR and pRL-TK. The cells were cultured for 43 h with vehicle and 10 nM testosterone in the absence or presence of various concentrations of nilutamide, and luciferase activity was measured. Firefly luciferase activity was normalized to *Renilla* luciferase activity. Each column represents the mean ± SE of three independent experiments. $^*p < 0.05$, significantly different from testosterone (+) in the absence of nilutamide.

promoter region. The ARE located furthest from the transcriptional start site was designated ARE-1 and that located closest was designated ARE-5. To determine which region(s) in the 5′-flanking region of rOCT2 gene is involved in expressional regulation by testosterone, constructs with deletions of the 5′-flanking region of rOCT2 gene were prepared and their luciferase activities were measured (Fig. 6). On deletion upstream to position −819, there was no induction by testosterone, suggesting that ARE-5 is not involved in the testosterone induction. But, on deletion up to position −1895, testosterone produced a 2-fold increase in activity, indicating that ARE-3 and/or -4 may work as response element(s). Furthermore, as the full-length promoter showed a 3-fold increase in activity, ARE-1 and/or -2 may also function as response elements.

To identify the functional sites for AR's activation, each ARE was mutated. As AR binds to specific response elements organized as an imperfect palindrome sequence (GGTACA nnnTGTTCT), we decided that the 3 bp at position 10–12 were changed to GCC in this sequence because left half-site of ARE is important for androgen receptor and ARE interaction (21). The promoter activity of rOCT2 with a mutation in each ARE revealed that mutated constructs of ARE-1 and ARE-3 were not affected by testosterone (Fig. 7). The other mutated constructs exhibited promoter activity to various extents in response to testosterone. These findings suggested that ARE-1 and ARE-3 play important roles in the activation of the rOCT2 promoter by testosterone.

DISCUSSION

Previously, we and others reported that the expression of rOCT2 mRNA in the kidney differed with gender, but neither rOCT1 nor rOCT3 (11,22), and that exogenous testosterone significantly stimulated only rOCT2 expression in the kidney of both male and female rats (12,23). Serum levels of testosterone were increased to about 1 μM in testosterone-administered rats. In the present study, we demonstrated that rOCT2 promoter activity was stimulated by 1 μM testosterone, whereas rOCT1 and rOCT3 promoters were not (Fig. 2B). These results are consistent with previous *in vivo* findings. 5′-Flanking region about 3000 bp of rOCT2 gene contained five putative AREs. The reporter assay using a series of deletion constructs and mutant constructs for each ARE revealed that ARE-1 (−2975 to −2960) and ARE-3 (−1340 to −1325), which have more similarity to the ARE consensus sequence than any other region, were responsible for the stimulation of rOCT2 promoter activity by testosterone (Figs. 6–7). As the promoter regions of rOCT1 and rOCT3 used in the present study do not have sequences highly homologous to ARE, the absence of an effect by testosterone on these two promoters is reasonable.

It was reported that there was no gender difference in rOCT2 mRNA expression in organs such as the liver and cerebellum (22). This may be a result of the low basal levels of rOCT2 mRNA or of the weak expression of AR in these organs compared to the kidney (24). We previously demonstrated that rOCT2 is predominantly expressed in the kidney, suggesting that some unidentified kidney-specific transcription factors cooperate to stimulate the rOCT2 promoter activity in the presence of testosterone. HEK293 cells (a human embryo kidney cell line) did not show any organic transporter activity (25). When HEK293 cells were used to measure rOCT2 promoter activity in the presence of AR and testosterone, there was no stimulative effect by testosterone (data not shown). It is probable that LLC-PK$_1$ cells express some transcription factor(s) necessary to express organic cation transporters. Further studies are needed to identify the kidney-specific transcription factors required for rOCT2 expression.

Other transporters have gender differences. For example, the level of rat organic anion transporter 2 (rOAT2) mRNA in the kidney and liver is higher in female than male rats (26,27), and the level of rOAT3 mRNA in male kidney is higher than

Table II. Comparison of the AREs in the Rat OCT2 Promoter Region

Position	Sequence	Homology (%)
ARE consensus	5′-**GGTACAnnnTGTTCT**-3′	-
ARE-1 (−2975 to −2960)	5′-**GGTAGAggaAGCTCT**-3′	80
ARE-3 (−1340 to −1325)	5′-**GGCACAggaTGCTCT**-3′	87
ARE-4 (−1268 to −1253)	5′-**GATACAgacTGTACC**-3′	80
ARE-5 (−548 to −533)	5′-**GAGACTaccTGTTTC**-3′	73

OCT = organic cation transporter.

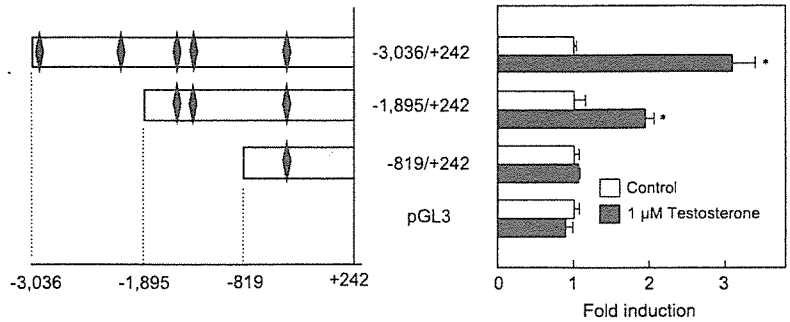

Fig. 6. *Trans*-activation of serial deletions of the rOCT2 promoter by rAR in the presence of testosterone. Various deletion constructs [equimolar amounts of the −3036/+242 construct (0.6 μg)] were transiently transfected into LLC-PK_1 cells with rAR and pRL-TK. The cells were cultured for 43 h with vehicle or 1 μM testosterone, and luciferase activity was measured. Firefly luciferase activity was normalized to *Renilla* luciferase activity. Black diamonds indicate AREs. Each column represents the mean ± SE of three independent experiments. $^*p < 0.05$, significantly different from control.

in females (27). Also, gender differences in rat renal cortical OAT1 and OAT3 levels (male > female) are caused by a stimulatory effect of androgens (28). Recently, Ohtsuki *et al.* (29) demonstrated that the expression of OAT3 in rat brain capillary endothelial cells was regulated by testosterone. Although Ohtsuki *et al.* (29) did not carry out reporter assay, it is conceivable that the expressions of the rOAT1 and rOAT3 genes are mediated by the interaction of AR and ARE on these promoters. The present study will be helpful to clarify transcriptional mechanisms of the induction of promoter activities of rOAT1 and rOAT3 by testosterone.

In humans, an evidence is the accumulation of gender differences in the efficacy and toxicity of drugs, and it is thought that physiological factors including body weight, plasma volume, and gastric emptying time are responsible for the variation in drug sensitivity between men and women (30). Recent studies have revealed that other differences, such as cytochrome P450 (CYP), cause gender-related variations in the pharmacokinetics of drugs. It is known that erythromycin (31), nifedipine (32), and verapamil (33), which are metabolized by CYP3A, have greater clearance in women than men. A sex-based difference in the expression of CYP3A4 was detected in the liver (34), but not in the intestine (35). In the renal clearance, amantadine and pramipexole, which are transported by OCT2 (36,37), also exhibit a gender difference (38,39). The renal clearance of amantadine was greater in men than women and was significantly reduced by quinine and quinidine only in men (40). In contrast, the pharmacokinetic parameters of cimetidine and procainamide do not differ between the sexes (41). It is noted that because the luminal efflux may be a rate-limiting step for renal secretion of organic cations (42), large differences in expression of a basolateral human (h)OCT2 may not result in similar large differences in renal clearance. There are some putative AREs in the promoter region of hOCT2, but the positions and sequences are different from those of rOCT2. Further studies are needed to clarify whether the expression of hOCT2 differs with gender, and whether the hOCT2 promoter interacts with the human androgen receptor.

In conclusion, a physiological concentration of testosterone (~10 nM) specifically enhanced transcription of rOCT2 gene, but not of rOCT1 or rOCT3 genes. ARE-1 (−2975 to

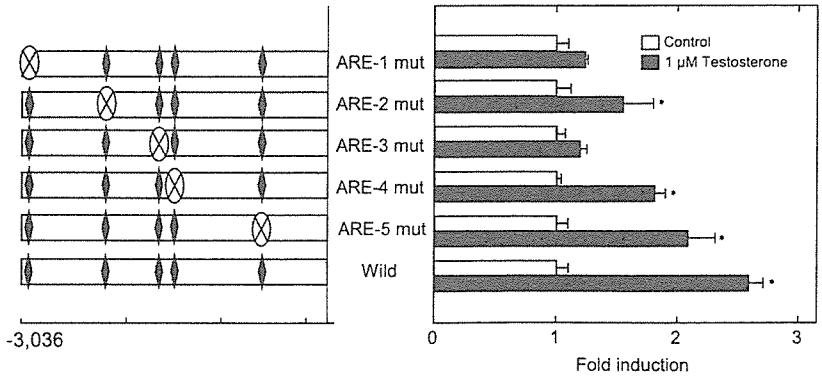

Fig. 7. *Trans*-activation of ARE-mutated rOCT2 promoters by rAR in the presence of testosterone. Constructs were transiently transfected into LLC-PK_1 cells with rAR and pRL-TK. The cells were cultured for 43 h with vehicle or 1 μM testosterone, and luciferase activity was measured. Firefly luciferase activity was normalized to *Renilla* luciferase activity. Black diamonds indicated AREs. Each column represents the mean ± SE of three independent experiments. $^*p < 0.05$, significantly different from control.

−2960) and ARE-3 (−1340 to −1325) in the rOCT2 promoter region would play important roles for the enhanced transcription of rOCT2 gene. These findings would account for the transcriptional mechanisms underlying the gender difference in the renal expression of rOCT2 and provide useful information to understand the renal handling of organic cations.

ACKNOWLEDGMENTS

This work was supported in part by the 21st Century COE program "Knowledge Information Infrastructure for Genome Science," a Grant-in-Aid for Scientific Research from the Ministry of Education, Culture, Sports, Science and Technology of Japan, and a Grant-in-Aid for Research on Advanced Medical Technology from the Ministry of Health, Labor and Welfare of Japan. J.A. is supported as a research assistant by the 21st Century COE program "Knowledge Information Infrastructure for Genome Science."

REFERENCES

1. K. Inui and M. Okuda. Cellular and molecular mechanisms of renal tubular secretion of organic anions and cations. *Clin. Exp. Nephrol.* **2**:100–108 (1998).
2. K. Inui, S. Masuda, and H. Saito. Cellular and molecular aspects of drug transport in the kidney. *Kidney Int.* **58**:944–958 (2000).
3. J. W. Jonker and A. H. Schinkel. Pharmacological and physiological functions of the polyspecific organic cation transporters: OCT1, 2, and 3 (SLC22A1–3). *J. Pharmacol. Exp. Ther.* **308**:2–9 (2004).
4. D. Gründemann, V. Gorboulev, S. Gambaryan, M. Veyhl, and H. Koepsell. Drug excretion mediated by a new prototype of polyspecific transporter. *Nature* **372**:549–552 (1994).
5. M. Okuda, H. Saito, Y. Urakami, M. Takano, and K. Inui. cDNA cloning and functional expression of a novel rat kidney organic cation transporter, OCT2. *Biochem. Biophys. Res. Commun.* **224**:500–507 (1996).
6. U. Karbach, J. Kricke, F. Meyer-Wentrup, V. Gorboulev, C. Volk, D. Loffing-Cueni, B. Kaissling, S. Bachmann, and H. Koepsell. Localization of organic cation transporters OCT1 and OCT2 in rat kidney. *Am. J. Physiol. Renal Physiol.* **279**: F679–F687 (2000).
7. M. Sugawara-Yokoo, Y. Urakami, H. Koyama, K. Fujikura, S. Masuda, H. Saito, T. Naruse, K. Inui, and K. Takata. Differential localization of organic cation transporters rOCT1 and rOCT2 in the basolateral membrane of rat kidney proximal tubules. *Histochem. Cell Biol.* **114**:175–180 (2000).
8. R. Kekuda, P. D. Prasad, X. Wu, H. Wang, Y. J. Fei, F. H. Leibach, and V. Ganapathy. Cloning and functional characterization of a potential-sensitive, polyspecific organic cation transporter (OCT3) most abundantly expressed in placenta. *J. Biol. Chem.* **273**:15971–15979 (1998).
9. Y. Urakami, M. Okuda, S. Masuda, M. Akazawa, H. Saito, and K. Inui. Distinct characteristics of organic cation transporters, OCT1 and OCT2, in the basolateral membrane of renal tubules. *Pharm. Res.* **18**:1528–1534 (2001).
10. H. M. Bowman and J. B. Hook. Sex differences in organic ion transport by rat kidney. *Proc. Soc. Exp. Biol. Med.* **141**:258–262 (1972).
11. Y. Urakami, N. Nakamura, K. Takahashi, M. Okuda, H. Saito, Y. Hashimoto, and K. Inui. Gender differences in expression of organic cation transporter OCT2 in rat kidney. *FEBS Lett.* **461**:339–342 (1999).
12. Y. Urakami, M. Okuda, H. Saito, and K. Inui. Hormonal regulation of organic cation transporter OCT2 expression in rat kidney. *FEBS Lett.* **473**:173–176 (2000).
13. H. J. Lee and C. Chang. Recent advances in androgen receptor action. *Cell. Mol. Life Sci.* **60**:1613–1622 (2003).
14. J. A. Tan, K. B. Marschke, K. C. Ho, S. T. Perry, E. M. Wilson, and F. S. French. Response elements of the androgen-regulated C3 gene. *J. Biol. Chem.* **267**:4456–4466 (1992).
15. K. B. Cleutjens, C. C. van Eekelen, H. A. van der Korput, A. O. Brinkmann, and J. Trapman. Two androgen response regions cooperate in steroid hormone regulated activity of the prostate-specific antigen promoter. *J. Biol. Chem.* **271**:6379–6388 (1996).
16. H. Saito, M. Yamamoto, K. Inui, and R. Hori. Transcellular transport of organic cation across monolayers of kidney epithelial cell line LLC-PK. *Am. J. Physiol.* **262**:C59–C66 (1992).
17. Y. Urakami, N. Kimura, M. Okuda, S. Masuda, T. Katsura, and K. Inui. Transcellular transport of creatinine in renal tubular epithelial cell line LLC-PK1. *Drug Metab. Pharmacokinet.* **20**: 200–205 (2005).
18. D. Gründemann J. Babin-Ebell, F. Martel, N. Ording, A. Schmidt, and E. Schömig. Primary structure and functional expression of the apical organic cation transporter from kidney epithelial LLC-PK1 cells. *J. Biol. Chem.* **272**:10408–10413 (2005).
19. J. P. Deslypere, M. Young, J. D. Wilson, and M. J. McPhaul. Testosterone and 5 alpha-dihydrotestosterone interact differently with the androgen receptor to enhance transcription of the MMTV-CAT reporter gene. *Mol. Cell. Endocrinol.* **88**:15–22 (1992).
20. T. Battmann, C. Branche, F. Bouchoux, E. Cerede, D. Philibert, F. Goubet, G. Teutsch, and M. Gaillard-Kelly. Pharmacological profile of RU 58642, a potent systemic antiandrogen for the treatment of androgen-dependent disorders. *J. Steroid Biochem. Mol. Biol.* **64**:103–111 (1998).
21. K. Barbulescu, C. Geserick, I. Schuttke, W. D. Schleuning, and B. Haendler. New androgen response elements in the murine pem promoter mediate selective transactivation. *Mol. Endocrinol.* **15**:1803–1816 (2001).
22. A. L. Slitt, N. J. Cherrington, D. P. Hartley, T. M. Leazer, and C. D. Klaassen. Tissue distribution and renal developmental changes in rat organic cation transporter mRNA levels. *Drug Metab. Dispos.* **30**:212–219 (2002).
23. L. Ji, S. Masuda, H. Saito, and K. Inui. Down-regulation of rat organic cation transporter rOCT2 by 5/6 nephrectomy. *Kidney Int.* **62**:514–524 (2002).
24. H. Takeda, G. Chodak, S. Mutchnik, T. Nakamoto, and C. Chang. Immunohistochemical localization of androgen receptors with mono-and polyclonal antibodies to androgen receptor. *J. Endocrinol.* **126**:17–25 (1990).
25. Y. Urakami, M. Akazawa, H. Saito, M. Okuda, and K. Inui. cDNA cloning, functional characterization, and tissue distribution of an alternatively spliced variant of organic cation transporter hOCT2 predominantly expressed in the human kidney. *J. Am. Soc. Nephrol.* **13**:1703–1710 (2002).
26. Y. Kato, K. Kuge, H. Kusuhara, P. J. Meier, and Y. Sugiyama. Gender difference in the urinary excretion of organic anions in rats. *J. Pharmacol. Exp. Ther.* **302**:483–489 (2002).
27. S. C. Buist, N. J. Cherrington, S. Choudhuri, D. P. Hartley, and C. D. Klaassen. Gender-specific and developmental influences on the expression of rat organic anion transporters. *J. Pharmacol. Exp. Ther.* **301**:145–151 (2002).
28. S. C. Buist, N. J. Cherrington, and C. D. Klaassen. Endocrine regulation of rat organic anion transporters. *Drug Metab. Dispos.* **31**:559–564 (2003).
29. S. Ohtsuki, M. Tomi, T. Hata, Y. Nagai, S. Hori, S. Mori, K. Hosoya, and T. Terasaki. Dominant expression of androgen receptors and their functional regulation of organic anion transporter 3 in rat brain capillary endothelial cells; comparison of gene expression between the blood–brain and –retinal barriers. *J. Cell. Physiol.* **204**:896–900 (2005).
30. J. B. Schwartz. The influence of sex on pharmacokinetics. *Clin. Pharmacokinet.* **42**:107–121 (2003).
31. C. M. Hunt, W. R. Westerkam, and G. M. Stave. Effect of age and gender on the activity of human hepatic CYP3A. *Biochem. Pharmacol.* **44**:275–283 (1992).
32. M. E. Krecic-Shepard, K. Park, C. Barnas, J. Slimko, D. R. Kerwin, and J. B. Schwartz. Race and sex influence clearance of nifedipine: results of a population study. *Clin. Pharmacol. Ther.* **68**:130–142 (2000).
33. K. Dilger, K. Eckhardt, U. Hofmann. K. Kucher. G. Mikus, and M. Eichelbaum. Chronopharmacology of intravenous and oral modified release verapamil. *Br. J. Clin. Pharmacol.* **47**:413–419 (1999).

34. R. Wolbold, K. Klein, O. Burk, A. K. Nussler, P. Neuhaus, M. Eichelbaum, M. Schwab, and U. M. Zanger. Sex is a major determinant of CYP3A4 expression in human liver. *Hepatology* **38**:978–988 (2003).
35. M. F. Paine, S. S. Ludington, M. L. Chen, P. W. Stewart, S. M. Huang, and P. B. Watkins. Do men and women differ in proximal small intestinal CYP3A or P-glycoprotein expression?. *Drug Metab. Dispos.* **33**:426–433 (2005).
36. A. E. Busch, U. Karbach, D. Miska, V. Gorboulev, A. Akhoundova, C. Volk, P. Arndt, J. C. Ulzheimer, M. S. Sonders, C. Baumann, S. Waldegger, F. Lang, and H. Koepsell. Human neurons express the polyspecific cation transporter hOCT2, which translocates monoamine neurotransmitters, amantadine, and memantine. *Mol. Pharmacol.* **54**:342–352 (1998).
37. N. Ishiguro, A. Saito, K. Yokoyama, M. Morikawa, T. Igarashi, and I. Tamai. Transport of the dopamine D2 agonist pramipexole by rat organic cation transporters OCT1 and OCT2 in kidney. *Drug Metab. Dispos.* **33**:495–499 (2005).
38. C. E. Wright, T. L. Sisson, A. K. Ichhpurani, and G. R. Peters. Steady-state pharmacokinetic properties of pramipexole in healthy volunteers. *J. Clin. Pharmacol.* **37**:520–525 (1997).
39. S. E. Gaudry, D. S. Sitar, D. D. Smyth, J. K. McKenzie, and F. Y. Aoki. Gender and age as factors in the inhibition of renal clearance of amantadine by quinine and quinidine. *Clin. Pharmacol. Ther.* **54**:23–27 (1993).
40. L. T. Wong, D. S. Sitar, and F. Y. Aoki. Chronic tobacco smoking and gender as variables affecting amantadine disposition in healthy subjects. *Br. J. Clin. Pharmacol.* **39**:81–84 (1995).
41. M. L. Chen, S. C. Lee, M. J. Ng, D. J. Schuirmann, L. J. Lesko, and R. L. Williams. Pharmacokinetic analysis of bioequivalence trials: implications for sex-related issues in clinical pharmacology and biopharmaceutics. *Clin. Pharmacol. Ther.* **68**:510–521 (2000).
42. S. H. Wright. Role of organic cation transporters in the renal handling of therapeutic agents and xenobiotics. *Toxicol. Appl. Pharmacol.* **204**:309–319 (2005).

BIOCHEMICAL PHARMACOLOGY 71 (2006) 1581–1588

available at www.sciencedirect.com

SCIENCE DIRECT®

journal homepage: www.elsevier.com/locate/biochempharm

The transcription factor Cdx2 regulates the intestine-specific expression of human peptide transporter 1 through functional interaction with Sp1

Jin Shimakura [a], *Tomohiro Terada* [a], *Yutaka Shimada* [b], *Toshiya Katsura* [a], *Ken-ichi Inui* [a,*]

[a] *Department of Pharmacy, Kyoto University Hospital, Faculty of Medicine, Kyoto University, Sakyo-ku, Kyoto 606-8507, Japan*
[b] *Surgery and Surgical Basic Science, Graduate School of Medicine, Kyoto University, Kyoto, Japan*

ARTICLE INFO

Article history:
Received 13 February 2006
Accepted 2 March 2006

Keywords:
PEPT1
Cdx2
Sp1
Transporter
Caco-2
Intestinal metaplasia

Abbreviations:
Cdx2, caudal-related homeobox protein 2
ChIP, chromatin immunoprecipitation
GAPDH, glyceraldehydes-3-phosphate dehydrogenase
HNF, hepatocyte nuclear factor
PEPT1, H+/peptide cotransporter 1
TBS, Tris-buffered saline

ABSTRACT

H^+/peptide cotransporter 1 (PEPT1, SLC15A1) localized at the brush-border membranes of intestinal epithelial cells plays important roles in the intestinal absorption of small peptides and a variety of peptidemimetic drugs. We previously demonstrated that transcription factor Sp1 functions as a basal transcriptional regulator of human PEPT1. However, the factor responsible for the intestine-specific expression of PEPT1 remains unknown. In the present study, we investigated the effect of the intestinal transcription factors on the transcription of the PEPT1 gene and found that only Cdx2 markedly trans-activated the PEPT1 promoter. However, the promoter region responsible for this effect lacked a typical Cdx2-binding sequence, but instead, possessed some Sp1-binding sites. In vitro experiments using Caco-2 cells showed that (1) mutation of the Sp1-binding site diminished the effect of Cdx2, (2) co-expression of Cdx2 and Sp1 synergistically trans-activated the PEPT1 promoter and (3) Sp1 protein was immunoprecipitated with Cdx2 protein. These results raise the possibility that Cdx2 modulates the PEPT1 promoter by interaction with Sp1. The significance of Cdx2 in vivo for PEPT1 regulation was shown by the determination of mRNA levels of Cdx2 and PEPT1 in human tissue. In gastric samples, some with intestinal metaplasia, the levels of PEPT1 and Cdx2 mRNA were highly correlated. Taken together, the present study suggests that Cdx2 plays a key role in the transcriptional regulation of the intestine-specific expression of PEPT1, possibly through interaction with Sp1.

1. Introduction

Di- and tripeptides are taken up into the intestinal and renal epithelial cells by H^+-coupled peptide transporters (PEPT1/SLC15A1 and PEPT2/SLC15A2). Many functional studies using heterologous expression systems have demonstrated molecular natures in their transport characteristics. For example, despite having similar substrate specificity, PEPT1 and PEPT2

* *Corresponding author.* Tel.: +81 75 751 3577; fax: +81 75 751 4207.
E-mail address: inui@kuhp.kyoto-u.ac.jp (K.-i. Inui).
0006-2952/$ – see front matter © 2006 Elsevier Inc. All rights reserved.
doi:10.1016/j.bcp.2006.03.001

were characterized as low- and high-affinity type transporters, respectively [1,2]. In addition, the two transporters differ in their tissue distribution and play distinct physiological roles. PEPT1 is expressed predominantly in the small intestine and slightly in the kidney [1,2]. On the other hand, PEPT2 is expressed mainly in the kidney, but it is also expressed in various tissues such as lung [3], choroid plexus [4] and mammary gland [5], and plays tissue-specific roles. As PEPT1 has broad substrate specificity, the intestinal absorption of several pharmacologically active drugs such as oral β-lactam antibiotics and the anti-viral agent valacyclovir are mediated by this transporter, and therefore, PEPT1 also plays important roles not only as a nutrient transporter but also as a drug transporter [2].

Previously, we isolated the promoter region of PEPT1 and demonstrated that the transcription factor Sp1 plays an important role in the basal transcriptional regulation of PEPT1 [6]. But, as Sp1 is expressed ubiquitously, the intestine-specific expression of PEPT1 cannot be controlled only by Sp1; thus, an intestine-restricted transcription factor is assumed to be involved.

The transcription factor Cdx2 is a member of the caudal-related homeobox gene family and expressed mainly in the intestine [7]. Cdx2 plays important roles in the early differentiation, proliferation and maintenance of intestinal epithelial cells [7,8], and in the transcription of intestinal genes, such as the sucrase–isomaltase [9], lactase–phlorizin hydrolase (LPH) [10], claudin-2 [11] and UDP glucuronosyl-transferases genes (UGTs) [12] through binding to a TTTAT/C consensus sequence. Over-expression of Cdx2 in undifferentiated rat IEC-6 intestinal epithelial cells leads to the development of a differentiated phenotype [8]. Furthermore, in humans, CDX2 has been reported to be associated with intestinal metaplasia in the stomach [13] in which ectopic expression of CDX2 is speculated to cause the gastric epithelial cells to trans-differentiate and take the intestinal phenotype. In our recent study, PEPT1 was also found to be expressed in the stomach, induced by intestinal metaplasia [14].

Considering the functions of Cdx2 mentioned above and overlapping of its expression with PEPT1, it is possible to suggest a link between these two genes. In the present study, we investigated the role of Cdx2 in the transcriptional regulation of PEPT1 using the human intestinal cell line Caco-2 cells. In addition, the correlation between PEPT1 and CDX2 mRNA expression levels in human gastric tissue samples developing intestinal metaplasia was also assessed.

2. Materials and methods

2.1. Materials

The anti-CDX2 monoclonal antibody was purchased from BioGenex (San Ramon, CA). The polyclonal antibody recognizing human Sp1 was from Upstate (Charlottesville, VA). The anti-FLAG M2 monoclonal antibody and anti-FLAG M2 monoclonal antibody conjugated to agarose gel (anti-FLAG M2 affinity gel) were obtained from Sigma (St. Louis, MO). The mouse Cdx2 expression vector (pRc/CMV-Cdx2) was a gift from Dr. Eun Ran Suh (University of Pennsylvania). The human HNF-1α and HNF-1β expression vectors were kindly supplied by Dr. Marco Pontoglio (Institute Pasteur, Paris, France). The CMV-Sp1 expression vector was kindly provided by Dr. Robert Tjian (University of California, Berkeley). The FLAG-Cdx2 expression plasmid was constructed by cloning the *Hin*dIII fragment of pRc/CMV-Cdx2 into pFLAG-CMV-6a (Sigma) at the *Hin*dIII restriction site. All other chemicals used were of the highest purity available.

2.2. Cloning of the 5′-regulatory region of PEPT1 gene and preparation of deletion reporter constructs

Cloning of the 5′-regulatory region of the PEPT1 gene and preparation of various reporter constructs were carried out as previously described [6]. Briefly, the 2940-bp flanking region upstream of the transcription start site was subcloned into the firefly luciferase reporter vector, pGL3-Basic (Promega, Madison, WI). This full-length reporter plasmid is hereafter referred to as −2940/+60. The 5′-deleted (−1111/+60, −960/+60, −401/+60, −247/+60, −172/+60 and −21/+60) constructs were generated by digestion of the −2940/+60 construct with the restriction enzymes. The −35/+60 construct was generated by PCR. Site-directed mutations in putative Sp1-binding sites were introduced into the −172/+60 construct with a Quik Change XL site-directed mutagenesis kit (Stratagene, La Jolla, CA).

2.3. Cell culture, transfection and reporter gene assay

Caco-2 cells were obtained from the American Type Culture Collection (ATCC CRL-1392) and maintained in Dulbecco's modified Eagle's medium supplemented with 10% fetal bovine serum and 1% non-essential amino acids. Caco-2 cells were plated into 24-well plates (3×10^5 cells/well) and transfected the following day with the reporter constructs, the expression plasmid for the transcription factor and 2.5 ng of the *Renilla reniformis* vector, pRL-TK (Promega), using Lipofectamine 2000 (Invitrogen Japan KK, Tokyo, Japan) according to the manufacturer's recommendations. The medium was changed after 24 h. The firefly and *Renilla* activities were determined 48 h after the transfection using a dual luciferase assay kit (Promega) and a LB940 luminometer (Berthold, Bad Wildbad, Germany). For the immunoprecipitation and chromatin immunoprecipitation experiments, Caco-2 cells were plated into 60-mm dishes (1.2×10^6 cells/dish) and transfected the following day with the expression plasmid for FLAG-Cdx2 using Lipofectamine 2000.

2.4. Immunoprecipitation and Western blotting

Caco-2 cells expressing FLAG-Cdx2 were washed with PBS twice, scraped off, and suspended in lysis buffer (50 mM Tris–HCl (pH 7.5), 150 mM NaCl, 1% Nonidet P-40, 0.5% sodium deoxycholate, 0.5 mM PMSF and 1% protease inhibitor cocktail (Nacalai tesque, Kyoto, Japan)). After an incubation at 4 °C for 15 min, the cells were disrupted by vigorous vortexing and repeated passages through a 24-gauge needle. The homogenate was centrifuged at 4 °C and 20,000 ×*g* for 10 min, and the supernatant was recovered. Immunoprecipitation of FLAG-Cdx2 was performed using anti-FLAG affinity gel at 4 °C overnight. The gel was washed with the lysis buffer five times. The immunoprecipitated FLAG-Cdx2 proteins were solubilized

in SDS sample buffer, separated on a 10% polyacrylamide gel at room temperature, and transferred onto polyvinylidene difluoride membranes (Immobilon-P; Millipore, Bedford, MA) by semidry electroblotting. Blots were blocked with 5% nonfat dry milk in Tris-buffered saline (TBS; 20 mM Tris, 137 mM NaCl, pH 7.5) with 0.1% Tween 20 (TBS-T) for 3 h at room temperature. The blots were washed in TBS-T and then incubated with the anti-FLAG M2 monoclonal antibody (10 μg/ml, 1 h at room temperature) or anti-Sp1 polyclonal antibody (1 μg/ml, overnight at 4 °C). Blots were washed three times with TBS-T, and the bound antibody was detected on X-ray film by enhanced chemiluminescence with a horseradish peroxidase-conjugated anti-mouse or anti-rabbit IgG antibody (Amersham Pharmacia Biotech, Piscataway, NJ).

2.5. *Chromatin immunoprecipitation (ChIP)*

Caco-2 cells expressing FLAG-Cdx2 were cross-linked with 1% formaldehyde at room temperature for 10 min. Cells then were rinsed with ice-cold PBS twice, scraped off, and suspended in lysis buffer (50 mM Tris–HCl (pH 7.5), 150 mM NaCl, 1% Nonidet P-40, 0.5% sodium deoxycholate, 0.5 mM PMSF and 1% protease inhibitor cocktail). Cells were sonicated three times for 15 s each time at 40% of the maximal setting (VP-5S, TAITEC, Koshigaya, Japan) and centrifuged at 4 °C and 20,000 ×*g* for 10 min. After the supernatants were collected and diluted in lysis buffer, immunoprecipitation was performed overnight at 4 °C with anti-FLAG affinity gel. The gel was then washed five times with lysis buffer and extracted with 1.5% SDS, followed by 0.5% SDS. Eluates were pooled and heated at 68 °C for 6 h to reverse the formaldehyde cross-linking. Chromatin-associated proteins were digested with proteinase K at 55 °C. The DNA was recovered by phenol–chloroform extraction and ethanol precipitation. Pellets were dissolved in 20 μl of TE buffer and used as a template for PCR. Primers used for amplifying the PEPT1 promoter were 5′-GACTGGCTCTCCCCCGGCCTGCCACG-3′ and 5′-CCCGGCCCCGTTGCCCCAGGTACAGC-3′ (−209 to −26 upstream of the transcriptional start site). PCR was performed using Advantage GC Genomic Polymerase Mix (BD Biosciences, Franklin Lakes, NJ) and cycling conditions were as follows: 1 min of denaturation at 95 °C, followed by 30 cycles of 30 s of denaturation at 94 °C, 3 min of primer annealing and extension at 68 °C, and 3 min of final extension at 68 °C.

2.6. *Human gastric tissue sample*

The gastric mucosal samples from normal stomachs were obtained from cancer patients ($n = 30$) during surgery at the First Department of Surgery, Kyoto University Hospital. Normal mucosal samples were resected at the site most distant from the affected portions. Three samples from different portions were resected in some patients. Pathologists diagnosed intestinal metaplasia in some patients. No patients underwent preoperative chemotherapy and/or radiation therapy. The samples were frozen in liquid nitrogen and stored at −80 °C until RNA extraction. This study was conducted in accordance with the Declaration of Helsinki and its amendments, and was approved by the Ethics Committee of Kyoto University (G-39). Written informed consent was obtained from all patients for surgery and the use of their resected samples.

2.7. *Real-time PCR*

Isolation of total RNA from the human stomach samples and real-time PCR were carried out as described previously [14]. The primer–probe set used for CDX2 was pre-developed TaqMan Assay Reagents (Applied Biosystems, Foster, CA). Glyceraldehydes-3-phosphate dehydrogenase (GAPDH) mRNA was also measured as an internal control with GAPDH Control Reagent (Applied Biosystems).

2.8. *Data analysis*

The results were expressed relative to the result obtained with the pGL3-Basic vector set as 1 and represent the means ± S.E. ($n = 3$). Two or three experiments were conducted, and representative results were shown. In the mutational experiment, statistical analysis was performed with the one-way ANOVA followed by Scheffé F post hoc testing.

3. Results

3.1. *Cdx2 activates transcription of the PEPT1 promoter–reporter construct*

To investigate whether Cdx2 activates the PEPT1 promoter, the −2940/+60 reporter construct was transiently transfected into Caco-2 cells simultaneously with Cdx2 expression plasmids. Besides Cdx2, the transcription factor hepatocyte nuclear factor (HNF)-1α is also expressed in the intestine and involved in the expression of some intestinal genes although it was first discovered in the liver [15,16]. In the regulation of LPH expression, Cdx2 is reported to directly interact with HNF-1α [10]. Thus, the effect of HNF-1α and a related transcription factor, HNF-1β, on the PEPT1 promoter was also assessed. Cdx2 over-expression resulted in a four-fold increase in promoter activity (Fig. 1). However, HNF-1α could neither activate the PEPT1 promoter nor enhance its activity driven by Cdx2. HNF-1β could activate it only a little as compared to Cdx2. Thus, we focused on Cdx2 as a possible regulator of PEPT1 expression and further investigated the Cdx2-responsive region in the PEPT1 promoter.

3.2. *Cdx2-responsive region located near the Sp1-binding sites*

To determine the elements contributing to the expression of PEPT1, we carried out a promoter 5′-deletion analysis (Fig. 2). The promoter activity in the absence of Cdx2 was strongest with the −401/+60 construct and gradually decreased by the deletion between −401 and −35, consistent with our previous result [6]. The promoter activity in the presence of Cdx2 increased three- to four-fold as compared to that in the absence of Cdx2 with the −2940 to −172 constructs whereas it was completely diminished with the −35/+60 construct, suggesting that the Cdx2-responsive region is located between −172 and −35. Unexpectedly, this region lacked a consensus Cdx2-binding site but contained multiple Sp1-binding sites as reported previously [6]. We could not find any transcription factor-binding sites which are likely to be responsible for the

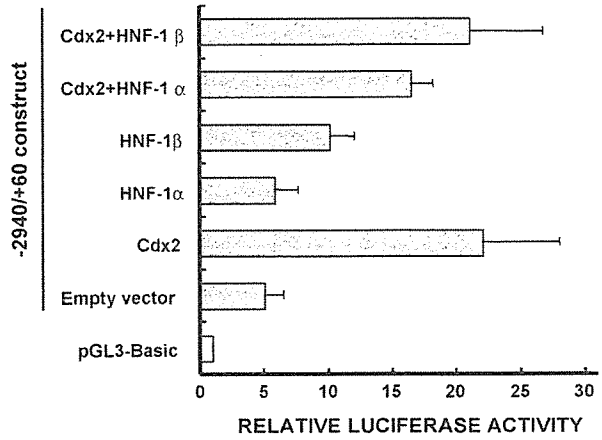

Fig. 1 – Effects of Cdx2, HNF-1α and HNF-1β over-expression on the PEPT1 promoter activity. Caco-2 cells were transiently transfected with 250 ng of the −2940/+60 construct and 250 ng of the expression vector for Cdx2, HNF-1α or HNF-1β. The total amount of transfected DNA (750 ng) was kept constant by adding empty vector. Firefly luciferase activity was normalized to *Renilla* luciferase activity. Data are reported as the relative fold-increase compared with pGL3-Basic and represent the mean ± S.E. ($n = 3$).

effect of Cdx2 except for Sp1 in this region. We next carried out a mutational analysis to determine whether the effect of Cdx2 was mediated through these Sp1-binding sites. The promoter activity in the absence of Cdx2 was reduced with the mutation of Sp-A, Sp-B or Sp-C sites, consistent with our prior study [6]. Trans-activation by Cdx2 was markedly decreased with the construct possessing the mutation of Sp-A or Sp-C sites (Fig. 3). These deletion and mutational analyses collectively suggest that Cdx2 may functions via interaction with Sp1 on the PEPT1 promoter.

3.3. *PEPT1 promoter was synergistically activated by Cdx2 and Sp1*

Sp1 has been shown to trans-activate the PEPT1 promoter [6]. We therefore determined whether Cdx2 enhances the promoter activity in cooperation with Sp1. Cdx2 or Sp1 alone caused a 1.5–2-fold increase of the promoter activity, whereas co-expression of Cdx2 and Sp1 resulted in a four-fold increase in the promoter activity (Fig. 4), suggesting a synergistic effect.

3.4. *Protein–protein interaction of Cdx2 and Sp1*

The synergistic effect of Cdx2 and Sp1 observed in the co-expression experiment, together with the observations from the mutational analysis, raise the possibility that these two proteins interact physically to regulate PEPT1 expression. We therefore investigated the interaction of Cdx2 and Sp1 within the cell using co-immunoprecipitation. Whole-cell extracts of Caco-2 cells transfected with the expression vector for FLAG-Cdx2 or empty vector were subjected to immunoprecipitation followed by Western blotting. Detection with anti-FLAG antibody confirmed that FLAG-Cdx2 protein was expressed in the cells transfected with FLAG-Cdx2 and appropriately immunoprecipitated (Fig. 5, upper panel). In the input samples, as expected, the band of Sp1 protein was detected both in the cells transfected with FLAG-Cdx2 and empty vector, while in the immunoprecipitated sample, it was detected only in the FLAG-Cdx2 transfected cells (Fig. 5, lower panel). These findings show that endogenous Sp1 protein was co-immunoprecipitated with FLAG-Cdx2 and suggest that Cdx2 and Sp1 were associated in a protein complex in Caco-2 cells.

3.5. *Cdx2 associates with the PEPT1 promoter*

As mentioned above, the Cdx2-responsive region lacked a consensus Cdx2-binding site, and an electrophoretic mobility shift assay failed to demonstrate the binding of Cdx2 with the PEPT1 promoter (data not shown). Thus we adopted an

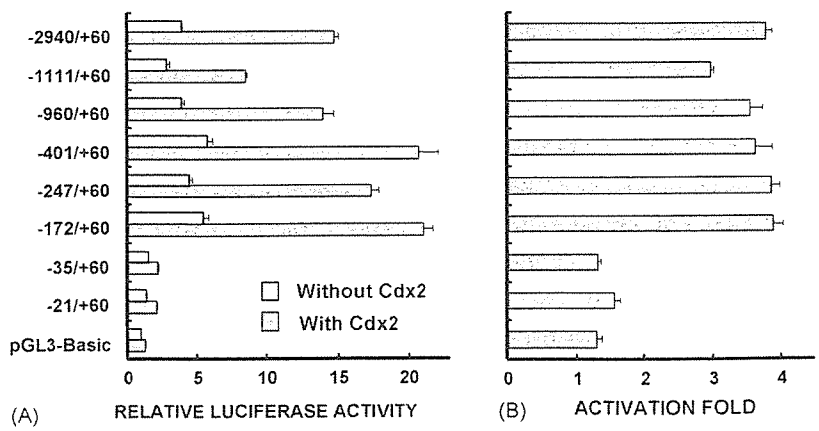

Fig. 2 – Identification of the Cdx2-responsive region in the PEPT1 promoter. A series of deleted promoter constructs (equimolar amounts of the −2940/+60 construct (500 ng)) and 500 ng of the Cdx2 expression vector or empty vector were transiently transfected into Caco-2 cells for luciferase assays. Firefly luciferase activity was normalized to *Renilla* luciferase activity. Data are reported as the relative fold-increase compared with the pGL3-Basic vector (A) or as the ratio of Cdx2-expressing vector to empty vector (B) and represent the mean ± S.E. ($n = 3$).